Variation in particulate C and N isotope composition following iron fertilization in two successive phytoplankton communities in the Southern Ocean

Gry Mine Berg,[1] Matthew M. Mills,[1] Matt C. Long,[1] Richard Bellerby,[2] Volker Strass,[3] Nicolas Savoye,[4,5] Rudiger Röttgers,[6] Peter L. Croot,[7,8] Adrian Webb,[9] and Kevin R. Arrigo[1]

Received 11 March 2011; revised 24 March 2011; accepted 25 April 2011; published 27 July 2011.

[1] Surface $\delta^{15}N_{PON}$ increased 3.92 ± 0.48‰ over the course of 20 days following additions of iron (Fe) to an eddy in close proximity to the Antarctic Polar Front in the Atlantic sector of the Southern Ocean. The change in $\delta^{15}N_{PON}$ was associated with an increase in the >20 μm size fraction, leading to a maximal difference of 6.23‰ between the >20 μm and <20 μm size fractions. Surface $\delta^{13}C_{POC}$ increased 1.18 ± 0.31‰ over the same period. After a decrease in particulate organic matter in the surface layer, a second phytoplankton community developed that accumulated less biomass, had a slower growth rate and was characterized by an offset of 1.56‰ in $\delta^{13}C_{POC}$ relative to the first community. During growth of the second community, surface $\delta^{13}C_{POC}$ further increased 0.83 ± 0.13‰. Here we speculate on ways that carboxylation, nitrogen assimilation, substrate pool enrichment and community composition may have contributed to the gradual increase in $\delta^{13}C_{POC}$ associated with phytoplankton biomass accumulation, as well as the systematic offset in $\delta^{13}C_{POC}$ between the two phytoplankton communities.

Citation: Berg, G. M., M. M. Mills, M. C. Long, R. Bellerby, V. Strass, N. Savoye, R. Röttgers, P. L. Croot, A. Webb, and K. R. Arrigo (2011), Variation in particulate C and N isotope composition following iron fertilization in two successive phytoplankton communities in the Southern Ocean, *Global Biogeochem. Cycles*, *25*, GB3013, doi:10.1029/2010GB003824.

1. Introduction

[2] The Southern Ocean, covering an area of 47×10^6 km^2, plays a key role in regulating Earth's climate [*Gille*, 2002; *Hansen et al.*, 2005]. Aided by cold temperatures, high wind speeds, and a high rate of CO_2 uptake by phytoplankton, up to 40% of the anthropogenic CO_2 stored in the global ocean transits through the Southern Ocean [*Caldeira and Duffy*, 2000; *Takahashi et al.*, 2002; *Mikaloff Fletcher et al.*, 2006; *Khatiwala et al.*, 2009]. In the present-day, iron (Fe) limits nutrient uptake by the phytoplankton community to 25% of the available surface macronutrient pool (e.g., nitrate), leaving 75% unused [*Sigman et al.*, 1999; *Sigman and Boyle*, 2000]. Given the tight coupling between nutrient utilization, productivity, and carbon fixation, the potential for increases in the drawdown of anthropogenic CO_2 is greater in the Southern Ocean than in any other oceanic region [*Marinov et al.*, 2006]. In fact, variation in Fe supply via dust deposition and upwelling to the Southern Ocean has been proposed to explain changes in the utilization of surface nutrients and the global changes in atmospheric CO_2 over glacial-interglacial cycles [*Martin*, 1990].

[3] Over the last 15 years, a number of experiments have taken place in the Southern Ocean to investigate the effects of artificial and natural Fe fertilization on aspects of ecosystem functioning, including biomass accumulation, productivity, CO_2 depletion, and carbon export [*Boyd et al.*, 2000; *Watson et al.*, 2000; *Gervais et al.*, 2002; *Coale et al.*, 2004; *Blain et al.*, 2007; *Seeyave et al.*, 2007; *Pollard et al.*, 2009]. The most recent of these investigations demonstrate a tight link between Fe supply and increased particle export, providing evidence that Fe fertilization does indeed affect the efficiency with which carbon trapped in particles formed at the surface are transported to depth [*Morris et al.*, 2007; *Savoye et al.*, 2008].

[4] While both artificial and natural Fe fertilization experiments stimulate phytoplankton growth, the precise

[1]Environmental Earth System Science, Stanford University, Stanford, California, USA.
[2]Bjerknes Center for Climate Research, University of Bergen, Bergen, Norway.
[3]Alfred Wegener Institute for Polar and Marine Research, Bremerhaven, Germany.
[4]UMR 5805 EPOC, Station Marine d'Arcachon, Université Bordeaux 1/CNRS, Arcachon, France.
[5]Department of Analytical and Environmental Chemistry, Vrije Universiteit Brussel, Brussels, Belgium.
[6]Forschungszentrum Geesthacht, Institut für Küstenforschung, Geesthacht, Germany.
[7]Insitut für Meereskunde-GEOMAR, Kiel, Germany.
[8]Now at Plymouth Marine Laboratory, Marine Biogeochemistry, Plymouth, UK.
[9]Oceanography Department, University of Cape Town, Rondebosch, South Africa.

0886-6236/11/2010GB003824

mechanism by which Fe stimulates productivity is not clear. Fe is a key cofactor in proteins involved in a number of biochemical reactions associated with both light harvesting and nitrogen assimilation. It is not clear which of these processes contribute most to phytoplankton growth and biomass increase upon relief of Fe starvation. For example, the photosynthetic apparatus is composed of several Fe-rich proteins including the photosystem I (PSI) reaction center protein, the cytochrome b_6f complex, and the electron acceptor ferredoxin. Under Fe starvation, cells adjust by substituting non-Fe containing proteins [*La Roche et al.*, 1996], and where substitution is not possible, by reducing the amount of Fe-rich proteins [*Strzepek and Harrison*, 2004]. This results in suboptimal functioning of the photosynthetic light reactions, including a lack of repair of damaged proteins, manifested in a depression of the photosystem II (PSII) quantum yield [*Greene et al.*, 1991] and the quantum yield of photosynthesis [*Hiscock et al.*, 2008]. To date, Fe addition experiments demonstrate that the quantum yield of PSII and the quantum yield of photosynthesis increase across all phytoplankton size classes with Fe addition [*Boyd*, 2002; *Hiscock et al.*, 2008]. This suggests that Fe additions should not favor growth of one species of phytoplankton over another, and that changes in species composition following Fe addition would be attributable to extrinsic factors such as grazing [*Assmy et al.*, 2007].

[5] Aside from the light reactions, Fe is a cofactor in the enzymes that reduce nitrate (NO_3^-) in the cell [*Raven*, 1988]. Because these cannot be substituted by non-Fe containing enzymes, Fe limitation results in a depression of NO_3^- assimilation [*Franck et al.*, 2003; *Timmermans et al.*, 2004]. In contrast with the community-wide effect of relieving the light harvesting system of Fe limitation, the effect of relieving NO_3^- reduction of Fe limitation is species-specific depending on the nitrogen (N) assimilation capabilities of the organism. Addition of Fe does not affect the growth of phytoplankton that lack the enzymes nitrate reductase and nitrite reductase which catalyze assimilatory NO_3^- reduction. These species depend on other sources of N, such as ammonium (NH_4^+) and urea [*Antia et al.*, 1975; *DeYoe and Suttle*, 1994; *Moore et al.*, 2002]. On the other end of the spectrum are species, mainly diatoms, that are specialized for growth on NO_3^- as evidenced by the coding of multiple, identical NO_3^- transporters in their genomes that are transcribed simultaneously into protein [*Hildebrand and Dahlin*, 2000; *Song and Ward*, 2007]. As such, diatoms benefit significantly from relief of iron limitation [*Price et al.*, 1991, 1994; *Timmermans et al.*, 2004].

[6] Knowing whether the biomass increase following Fe fertilization results primarily from increased light harvesting or from increased N uptake would tell us whether we could expect an increase in the growth of all phytoplankton species or in the growth of a few. In turn, this information may help us evaluate past records of phytoplankton biomass changes. Stable N isotope data from Southern Ocean sediment organic matter suggest that during the last glacial maximum (LGM), NO_3^- utilization was 2–4 times greater than it is today [*Francois et al.*, 1997; *Sigman et al.*, 1999]. The interpretation of these data assumes that the fractionation factor for NO_3^- uptake is the same across all phytoplankton species and that it has remained constant through time. More recent data suggest that fractionation during uptake of NO_3^- by small cells, primarily nondiatoms, is two times greater than in large, diatomaceous cells [*Karsh et al.*, 2003]. As such, increases in sedimentary ^{15}N content primarily driven by small, as opposed to large cells, would indicate that nutrient depletion during the LGM was significantly less than what is currently calculated based on present-day community composition dominated by larger cells [*Karsh et al.*, 2003].

[7] Examining changes in particulate ^{15}N content may provide mechanistic insight into how Fe stimulates phytoplankton growth. Typically, increased NO_3^- assimilation leads to an increase in the ^{15}N enrichment of dissolved NO_3^- and of particulate matter according to Rayleigh fractionation kinetics [*Altabet*, 1996; *DiFiore et al.*, 2006]. The Southern Ocean, and other high nutrient low chlorophyll (HNLC) regions, presents a special case as variation in particulate ^{15}N content is frequently uncoupled from variation in ^{15}N-NO_3^- [*Altabet*, 1996; *Karsh et al.*, 2003; *Needoba et al.*, 2006]. In this case, variation in particulate ^{15}N content may be attributable to a switch between NH_4^+ and NO_3^- assimilation mediated by Fe fertilization [*Needoba et al.*, 2006].

[8] Similar to the increase in particulate ^{15}N content, increases in particulate ^{13}C content following Fe fertilization have been documented [*Trull and Armand*, 2001; *Trull et al.*, 2008]. However, it is less straightforward to attribute the increase in ^{13}C to a switch in the inorganic carbon (C) source or to substrate pool enrichment. With respect to the former, a switch between bicarbonate (HCO_3^-) and CO_2(aq) as the primary C source is not likely to produce a variation in particulate ^{13}C because dehydration of HCO_3^- to CO_2(aq) via carbonic anhydrase (CA) has an associated isotope discrimination factor that is similar to the 10‰ isotopic difference between HCO_3^- and CO_2(aq). This means that cells which take up HCO_3^- as a substrate for CA will have the same isotopic composition as cells that rely primarily on CO_2(aq) diffusion [*Riebesell and Wolf-Gladrow*, 1995]. With respect to the latter, spontaneous and enzymatic interconversion between (HCO_3^-) and CO_2(aq) effectively makes the entire total dissolved inorganic carbon (DIC) pool available for phytoplankton uptake [*Tortell et al.*, 1997, 2008]. This pool is much greater than the C requirement of phytoplankton, therefore, changes in the ^{13}C enrichment of the DIC, as well as in CO_2(aq), are assumed to be negligible [cf. *Popp et al.*, 1989; *Rau et al.*, 1989; 1992; *Freeman and Hayes*, 1992]. However, in cases where phytoplankton growth is so rapid that CO_2(aq) is depleted at a rate faster than its rate of resupply, the isotopic composition of particulate matter may increase due to the progressive enrichment in ^{13}C of CO_2(aq) resulting from fractionation during CO_2 fixation [*Deuser*, 1970]. This is especially true for coastal regions with intense phytoplankton growth [*Villinski et al.*, 2008].

[9] To gain insight into the mechanisms behind Fe-induced increases in productivity, we examined simultaneous changes in the quantum yield of PSII (F_v/F_m), and the $^{15}N/^{14}N$ and $^{13}C/^{12}C$ ratios in suspended particulate matter during the European Iron Fertilization Experiment (EIFEX). We relied on high-resolution, daily sampling over a small region to look specifically at how changes in these three parameters covaried over the rise and fall of two successive biomass peaks induced by Fe fertilization. Variation in

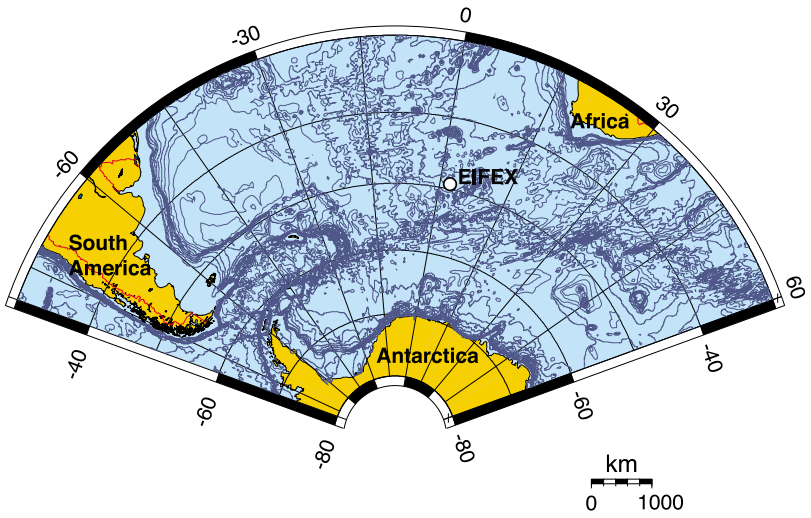

Figure 1. Location (2°15′E, 49°15′S) of EIFEX iron fertilization investigation in the Southern Ocean indicated by the white circle. Map generated using http://www.planiglobe.com/omc_set.html created by M. Weinelt.

particulate $^{15}N/^{14}N$ and $^{13}C/^{12}C$ ratios were related to changes in $^{15}N/^{14}N$ and $^{13}C/^{12}C$ ratios of dissolved pools based on known relationships between changes in dissolved N and C concentrations and isotope fractionation. Previous investigations that have measured simultaneous variation in N and C isotopic composition in suspended organic matter typically sample over large space and time scales, comparing different years or different locations [*Rau et al.*, 1990; *Trull et al.*, 2008; *Tamelander et al.*, 2009]. Here, we were fortunate to sample at timescales on par with phytoplankton generation times, in addition to sampling within the same population of cells over the course of a month. This allowed us to discriminate the effects of enrichment of the dissolved pool from effects related to phytoplankton cell physiology on particulate matter isotopic composition.

2. Materials and Methods

[10] The EIFEX Fe addition experiment was carried out in a cyclonic eddy approximately 100 km in diameter enclosed by a meander of the Antarctic Polar Front (at 2°15′E, 49°15′S) in the Atlantic sector of the Southern Ocean in January–March of 2004 (Figure 1). Due to the deep reach of the Antarctic Circumpolar Current, eddies formed from its meanders are vertically coherent from the surface mixed layer to the deep water column and provide a confined body of water within which responses to iron addition can be tracked [*Strass et al.*, 2005; *Cisewski et al.*, 2008]. The eddy was selected based on satellite altimeter data and located by mapping of its circulation pattern with an acoustic Doppler current profiler. On day 1 of the experiment, a patch of water in the core of the eddy was fertilized with 7000 kg of iron sulfate ($FeSO_4 \bullet 7H_2O$) dissolved in acidified seawater. The patch expanded from an initial area of 170 km^2 to approximately 540 km^2 by day 14, at which time it was fertilized with an additional 7000 kg of acidified $FeSO_4 \bullet 7H_2O$. By day 37 of the experiment, helicopter-mounted lidar mapping showed that the bloom covered >1000 km^2, or approximately one fifth of the area of the eddy. Dissolved Fe concentrations increased from a background value of 0.2 nmol L^{-1} to 2.2 nmol L^{-1} following the first fertilization event, then steadily decreased to 0.25 nmol L^{-1} by day 36 of the experiment (C. Schlosser et al., Influence of iron binding ligands on solubility in a mesoscale iron fertilization experiment (EIFeX) in the Southern Ocean, submitted to *Marine Chemistry*, 2010). Analysis of temperature-salinity data coupled with microstructure sensor-derived density and energy dissipation profiles revealed that the upper 40–60 m of the total mixed layer depth of the eddy was actively mixing [*Cisewski et al.*, 2008]. This actively mixed layer (AML) was distinguished by greater accumulations of particulate matter than the layer below which extended to the base of the total mixed layer (MLD) at 98 ± 20 m [*Cisewski et al.*, 2008]. Most of the biological activity recorded in the present investigation occurred in the AML.

[11] Aside from spreading and growing in size, the patch rotated around the eddy core completing a full rotation approximately once per week. Drift of the fertilized patch was tracked by a surface spar buoy drogued at 20–30 m. The buoy recorded and transmitted its position via GPS/Radio and GPS/ARGOS modules. The patch was also tracked by a helicopter-mounted chlorophyll fluorescence lidar. For details regarding eddy detection, mapping, and patch tracking, see *Strass et al*. [2005]. In addition to tracking by buoy and mapping by lidar, the patch was surveyed by following changes in the ratio of variable to maximal fluorescence (F_v/F_m) of the phytoplankton community. F_v/F_m was calculated according to the equation: $F_v/F_m = (F_m - F_0)/F_m$, where F_0 is the basal fluorescence level and F_m is the maximal fluorescence level following excitation at 470 nm. F_0 and F_m were determined with a Fast-Repetition-Rate-Fluorimeter (FRRF, FastTracka Instrument, Chelsea Instruments LTD) in flow-through mode with water intake at 11 m according to *Röttgers et al*. [2005]. Continuous depth profiles of F_0 and F_m from the surface down to 200 m were also recorded using a Rosette-mounted FastTracka. Data corresponding with discrete depth intervals were binned, and the binned

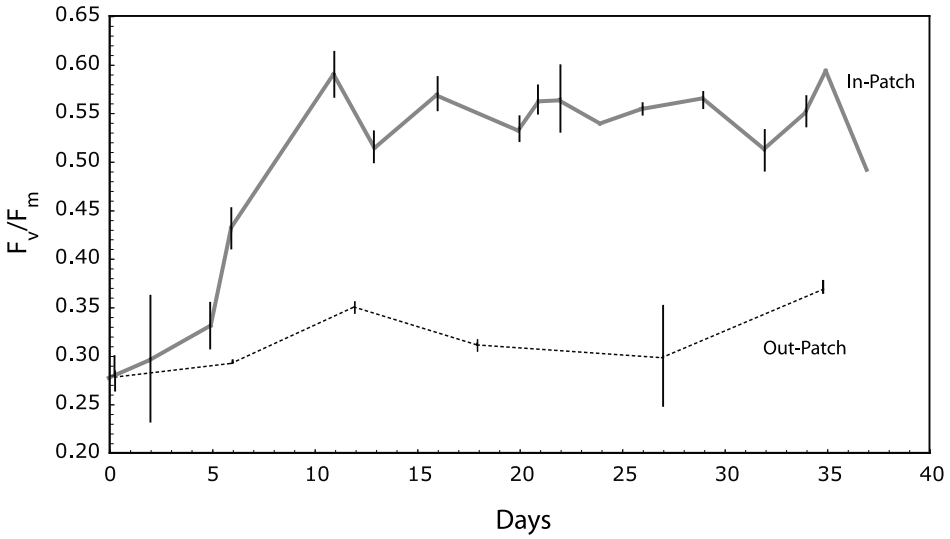

Figure 2. Discrete depth-binned and surface-averaged (10–40 m) F_v/F_m measurements from in-patch (gray line) and out-patch (dashed line) stations. Means and standard deviations of four depths are shown.

data for the top 40 m, corresponding with the AML, were averaged.

[12] Concentrations of dissolved N (NH_4^+, NO_3^-) were determined on board immediately following collection from CTD casts using a Technicon II autoanalyzer following standard methods. Discrete measurements of DIC were taken from CTD casts and analyzed within 24 h of collection. Total dissolved inorganic carbon (DIC) analyses were made by coulometric titration [*Johnson et al.*, 1987] using a SOMMA system calibrated against certified reference materials (CRM) from Dr. Andrew Dickson. The DIC measurement of CRM material generally agreed to better than 2 μmol kg^{-1}. CO_2 was computed from DIC and alkalinity using the methods recommended by *Dickson and Goyet* [1994].

[13] Samples for analysis of particulate organic carbon (POC) and nitrogen (PON) content, $\delta^{15}N_{PON}$ and $\delta^{13}C_{POC}$ were filtered from discrete depths between 5 and 200 m at in-patch and out-patch stations. Depending on the water column phytoplankton chlorophyll *a* (Chl *a*), 2–5 L of water was filtered through precombusted Whatman GF/F glass fiber filters. Large, visible zooplankton were removed from the filters. Whole water was also size-fractionated through 20 μm nylon mesh by gravity filtration. Both the particles that passed through the mesh and particles caught on the mesh (rinsed off with particle-free seawater) were subsequently filtered onto GF/F filters. All the GF/F filters were dried overnight at 50°C and stored dry in combusted glass Petri dishes until removal of inorganic C and mass spectrometer analysis. Inorganic C was removed prior to mass spec analysis according to *Lorrain et al*. [2003]. Briefly, the dried filters were exposed to HCl fumes for 4 h in a dessicator, followed by 3 h in a fume hood to drive off residual HCl, and drying in an oven at 60°C.

[14] POC, PON, $\delta^{13}C$ and $\delta^{15}N$ analysis of the particles on the filters was conducted using a Thermo Finnigan Delta plus mass spectrometer coupled with a Carlo Erba NA-1500 Series II elemental analyzer (EA) via a ConFLo II interface. All samples were packed in lightweight tin cups for analysis. The samples were combusted in a stream of oxygen at an oven temperature of 1,080°C in a quartz tube packed with silica chips, silver coated cobalt oxide and chromium oxide to yield N_xO_x and CO_2. The gas stream then passed over hot copper at 650°C to yield N_2 gas. Water was removed from the gas stream using an in-line water trap containing phosphorus pentoxide prior to the copper reduction. Acetanilide was used as the C and N mass calibration standard. The $\delta^{15}N$ and $\delta^{13}C$ isotopic compositions are expressed in delta notation versus atmospheric N_2 and Pee Dee Belemnite standard, respectively. Standardization was by reference to CO_2 and N_2 working gases injected in triplicate before each sample. Peptone calibrated against the N standards IAEA N1 and IAEA N3 and the C standard NBS-21 was used as the standard for $\delta^{15}N$ and $\delta^{13}C$, respectively, and run between every 6–8 samples. Reproducibility for $\delta^{13}C$ and $\delta^{15}N$ was better than 0.3‰. Mass isotope effects were corrected using the methods of *Avak and Fry* [1999]. Filter blanks were measured by passing 1 L filtered seawater through a GF/F filter which was dried, processed and measured as the sample filters. These filters yielded negligible amounts of POC and PON (<1% of typical samples) and no correction was applied.

3. Results and Discussion

[15] Of the biological variables followed in our investigation, F_v/F_m was the first parameter to respond following the initial fertilization event, starting to increase only four hours after fertilization. After the first five days, F_v/F_m was 54% higher than at time zero (t_0) and it remained elevated throughout the sampling period (Figure 2). F_v/F_m typically varies between 0.1 and 0.75 in marine eukaryotic phytoplankton depending on light acclimation and nutrient status of the cells [*Greene et al.*, 1991; *Geider et al.*, 1993]. In particular, Fe and nitrogen (N) limitation tend to reduce F_v/F_m through their control on chlorophyll synthesis and carbon (C) fixation [*Kolber et al.*, 1988; *La Roche et al.*, 1993; *Behrenfeld et al.*, 1996]. Relief from Fe and N

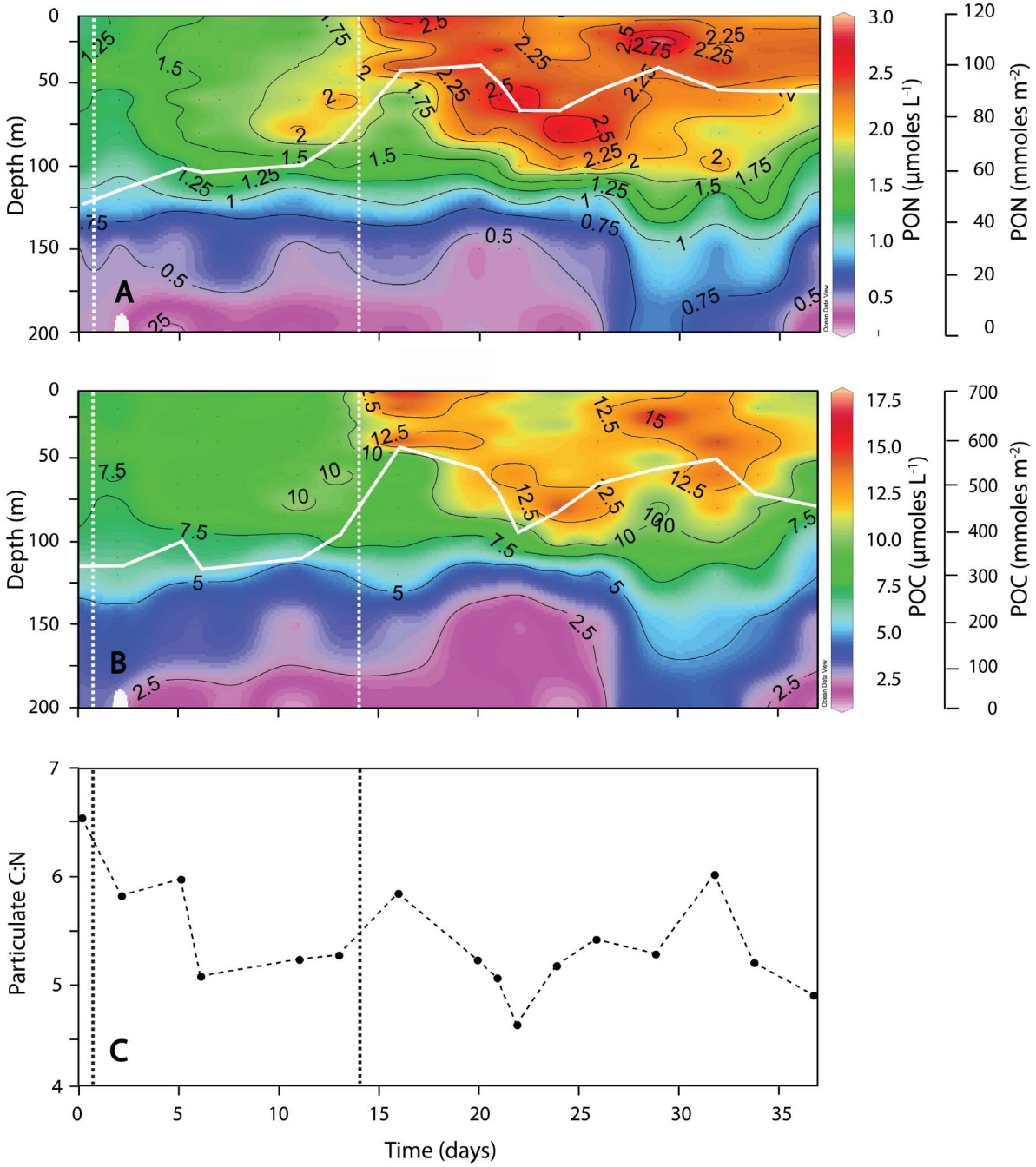

Figure 3. (a) Contour plot of PON concentration (μmol L^{-1}) with surface (top 40 m) depth-integrated PON concentration (mmol m^{-2}) superimposed in white solid line. (b) Contour plot of POC concentration (μmol L^{-1}) with surface depth-integrated POC concentration superimposed in white solid line. (c) Ratio of depth-integrated POC:PON. Dashed vertical lines represent days that iron additions took place.

limitation, and a subsequent increase in F_v/F_m, has been used as a sensitive measure to track Fe fertilization of natural phytoplankton communities [*Kolber et al.*, 1994; *Behrenfeld et al.*, 1996; *Coale et al.*, 1996; *Boyd et al.*, 1998, 2000; *Boyd and Abraham*, 2001; *Boyd*, 2002; *Moore et al.*, 2006]. Relief from Fe limitation was inferred from the difference in F_v/F_m between the in-patch and the out-patch stations, reaching a maximum difference of ~0.25 between days 11 and 12 which persisted throughout the duration of the experiment.

[16] Eleven days following fertilization, PON and POC concentrations started to increase, doubling by days 16–20 (Figures 3a and 3b). Chl *a* concentrations increased fivefold over the same time interval [*Hoffmann et al.*, 2006], driven by a more rapid increase in Chl *a* $cell^{-1}$ than POC $cell^{-1}$, as would be expected from a population of phytoplankton cells transitioning from nutrient limitation to nutrient sufficiency

[*La Roche et al.*, 1993; *Graziano et al.*, 1996]. After day 20, PON and POC concentrations declined in the upper 40 m of the water column while increasing below 60 m, indicating a settling of the particulate matter from the AML. Clumping of diatom aggregates drove the gradual sinking and accumulation of biomass between 60 and 100 m depth (P. Assmy et al., Species composition of an iron-fertilized phytoplankton bloom determines the fate of its biomass, manuscript in preparation, 2011). Light attenuation, recorded using a transmissometer (not shown here), gradually decreased in the AML during the time of slow settling. After a minimum was reached between days 22–24, concentrations of PON and POC once again started to increase in the AML and reached a new peak between days 29–32 (Figures 3a and 3b). Meanwhile, the aggregates that had accumulated at the bottom of the MLD (60–100 m) reached a critical mass and rapidly sank out on day 32, as evidenced by a sudden decrease in beam attenuation from the surface down to 1500 m (V. Smetacek et al., Massive carbon flux to the deep sea from an iron-fertilized phytoplankton bloom in the Southern Ocean, manuscript in preparation, 2011) and a sudden increase in POC export flux [*Jacquet et al.*, 2008; N. Savoye, unpublished data, 2004].

[17] Cell counts and analyses of pigment concentrations suggested that the surface layer peaks recorded on days 16–20 and 29–32 were dominated by two different phytoplankton assemblages [*Hoffmann et al.*, 2006; *Croot et al.*, 2007]. The first assemblage comprised a mixture of three *Chaetoceros* species >20 μm in size dominated by *Chaetoceros dichaeta* [*Croot et al.*, 2007]. The second assemblage consisted of cells 2–20 μm in size dominated by *Pseudo-nitzchia* sp., but also included *Fragilariopsis cylindrus*, the haptophyte *Phaeocystis antarctica*, and eukaryotic picoplankton [*Hoffmann et al.*, 2006; *Croot et al.*, 2007]. The *Pseudo-nitzchia* sp. population peaked on day 32 and decreased in concentration rapidly thereafter, leaving a community with a slightly different composition by day 37 of the experiment [*Croot et al.*, 2007].

[18] These two communities were clearly distinguished based on nutrient drawdown and growth rates. Accumulation of 50 mmol PON m^{-2} and 262 mmol POC m^{-2} in the AML during the first 16 days was balanced by the drawdown of 47 mmol NO_3^- m^{-2} and 339 mmol DIC m^{-2}. The depth-integrated DIC: NO_3^- disappearance ratio in the AML for this period was 7.2 (mol:mol) and the particulate C:N ratio (between days 13–16) was 5.2–5.8, down from 6.5 at t_0 (Figure 3c). The net community growth rate, calculated based on changes in POC, was 0.57 divisions d^{-1}. Between days 20–24, there was a marked decrease in particulate concentrations in the AML followed by a second increase in PON and POC. In contrast to the first 16 days of the experiment, PON and POC increases during the second biomass accumulation period (days 22–29) were smaller and the DIC: NO_3^- depth-integrated disappearance ratio was 13.7 (mol:mol), suggesting that two times more DIC was consumed per mole NO_3^- than during the first biomass increase. The net community growth rate during this period was 0.35 divisions d^{-1} and the particulate C:N ratio (between days 22–24) was 4.6–5.2 (Figure 3c). A C:N ratio consistently between 4.6 and 5.8 suggested to us that the samples were dominated by phytoplankton. However, these samples also contained small-sized zooplankton that did not change in abundance over the course of the experiment, therefore their contribution to the particulate signal was likely constant. In contrast, the large zooplankton size fraction, which we picked off the filters, changed fourfold over the course of our experiment [*Krägefsky et al.*, 2009; Assmy et al., manuscript in preparation, 2011]. In a similar comparison of nutrient drawdown ratios between two phytoplankton communities, *Arrigo et al.* [1999] noted a slightly greater DIC: NO_3^- disappearance ratio for diatom-dominated (9.2 ± 1.66) compared with *Phaeocystis antarctica* dominated (7.81 ± 1.32) waters. These ratios are closer to the disappearance ratio observed during the first, *Chaetoceros* dominated community, suggesting that the second, mixed phytoplankton community had a biochemical signature that differed significantly from communities dominated largely by fast growing diatoms or *P. antarctica*.

[19] PON accumulation post-Fe addition was relatively more enriched in $\delta^{15}N$ than the phytoplankton population that existed prior to Fe addition (Figure 4a). The depth-averaged difference between preenrichment and post-enrichment in $\delta^{15}N$ of the PON ($\delta^{15}N_{PON}$) was 3.92 ± 0.48‰ in the upper 40 m (Figure 4a). Relative to t_0, $\delta^{15}N_{PON}$ increased all the way down to the bottom of the mixed layer (100 m), which agreed well with the increase in PON throughout the mixed layer (Figure 4b). The depth-averaged $\delta^{15}N_{PON}$ difference declined to 2.05 ± 0.37‰ in the upper 40 m during the period of biomass decline (day 20–24). Moreover, this decline in $\delta^{15}N_{PON}$ persisted down to 100 m (Figure 4c) and contrasted with the depth distribution of the PON (Figure 4d). Whereas total depth-integrated PON in the upper 100 m was similar between day 20 and 24 (214 and 212 mmol m^{-2} respectively), 78% of this PON was distributed above 60 m on day 20 while only 45% of the PON was distributed above 60 m on day 24. From day 21 to 24, 33% of the PON had shifted from above to below 60 m. $\delta^{15}N_{PON}$ also decreased between 0 and 60 m suggesting the loss of a heavy $\delta^{15}N$ fraction (Figures 4c and 4d). However, this loss did not result in an increase in $\delta^{15}N_{PON}$ below 60 m during this same period (Figures 4c and 4d). *Chaetoceros* cells settling out of the AML-dominated PON accumulation from 60 to 100 m on day 24 (Assmy et al., manuscript in preparation, 2011).

[20] Mass balance calculations suggest that the PON that was lost from 0 to 60 m had a $\delta^{15}N$ value of 10.6‰, but that the material gained between 60 and 100 m had a $\delta^{15}N$ value of 0.31‰. The mechanism behind this unbalanced loss and gain in $\delta^{15}N$ is unclear. Production of enriched fecal material that settled out of the mixed layer, coupled with some selectivity in the PON downward transfer, is one possibility [*Altabet*, 1989; *Altabet and Small*, 1990]. Alternatively, nutrient limitation resulting in loss of membrane potential could lead to both settling of particles and leakage of intracellular N [*Agustí and Sanchez*, 2002; *Timmermans et al.*, 2007]. Leakage of N from the *Chaetoceros* subpopulation, although small in terms of N mass, could be significant in terms of $\delta^{15}N$. Loss of this N would likely not have a high fractionation factor as the net isotope effect of organic N degradation is small [*Sigman and Casciotti*, 2001]. Consistent with the scenario that N leaked from the settling cells, we noted a 20 mmol m^{-2} increase in NH_4^+ in the AML immediately following the start of the PON decline on day 20 that was quickly taken up in the following days. During

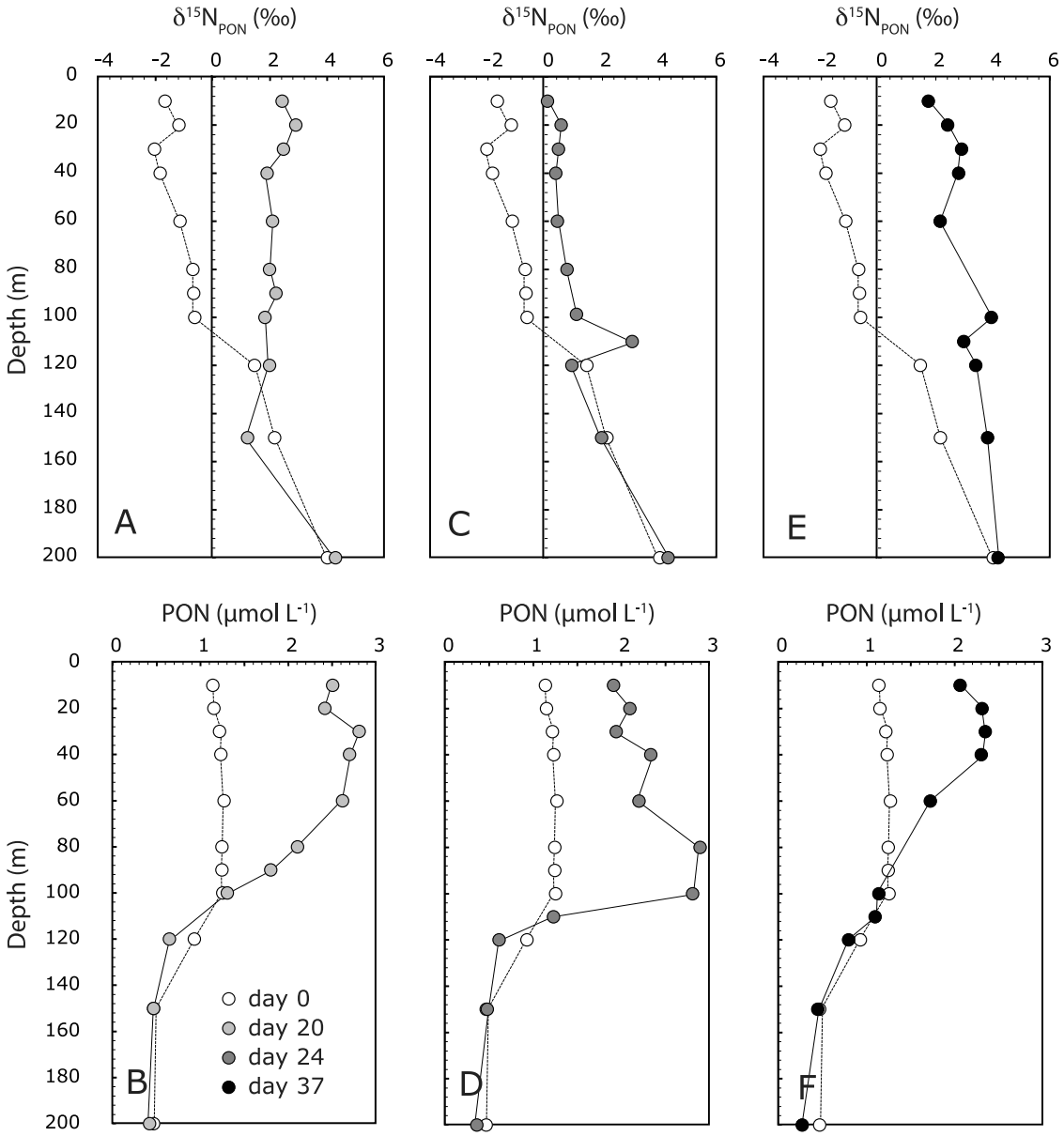

Figure 4. Comparative (a, c, e) $\delta^{15}N_{PON}$ and PON (b, d, f) depth profiles on day 0 (open circles), day 20 (light gray circles; first $\delta^{15}N_{PON}$ peak), day 24 (dark gray circles; $\delta^{15}N_{PON}$ minimum), and day 37 (black circles; second $\delta^{15}N_{PON}$ maximum).

the second, smaller increase in PON, depth-averaged $\delta^{15}N_{PON}$ increased 2.1 ± 0.38‰, similar in magnitude to the previous loss of ^{15}N from the particles, bringing the depth-averaged $\delta^{15}N_{PON}$ enrichment, relative to pre Fe addition, to 4.14 ± 0.75‰, the same level as the first bloom (Figures 4e and 4f).

[21] Depth-averaged $\delta^{13}C$ of the POC ($\delta^{13}C_{POC}$) in the AML increased 0.73 ± 0.18‰ during the first biomass increase relative to pre-Fe fertilization conditions (Figure 5a). POC distribution was similar to PON in the upper 100 m and corresponded with the increase in $\delta^{13}C_{POC}$ (Figure 5b). During the period of particle settling, depth-averaged $\delta^{13}C_{POC}$ decreased by 0.23 ± 0.23‰ (ns) in the AML while POC accumulated at 60–100 m (Figures 5c and 5d). During the second biomass increase, depth-averaged $\delta^{13}C_{POC}$ increased by 1.3 ± 0.27‰, increasing enrichment relative to pre-Fe addition by 1.82 ± 0.19‰. As with the increase in $\delta^{15}N_{PON}$, this increase in $\delta^{13}C_{POC}$ occurred without a concomitant increase in POC (Figures 5e and 5f). Relative to pre-Fe addition, there was a 2.5-fold difference in $\delta^{13}C_{POC}$ between the two biomass peaks. Given identical levels of $\delta^{15}N_{PON}$, the primary distinguishing factor between the two communities was the difference in the C isotopic enrichment.

[22] By regressing $\delta^{15}N_{PON}$ against $\delta^{13}C_{POC}$, we observed that the data fell along two main trend lines (Figure 6). Most of the samples corresponding to the first community (days 5–22) aligned along the lighter carbon trend line whereas most of the sampling points corresponding to the second community (days 29–37) aligned along the heavier carbon

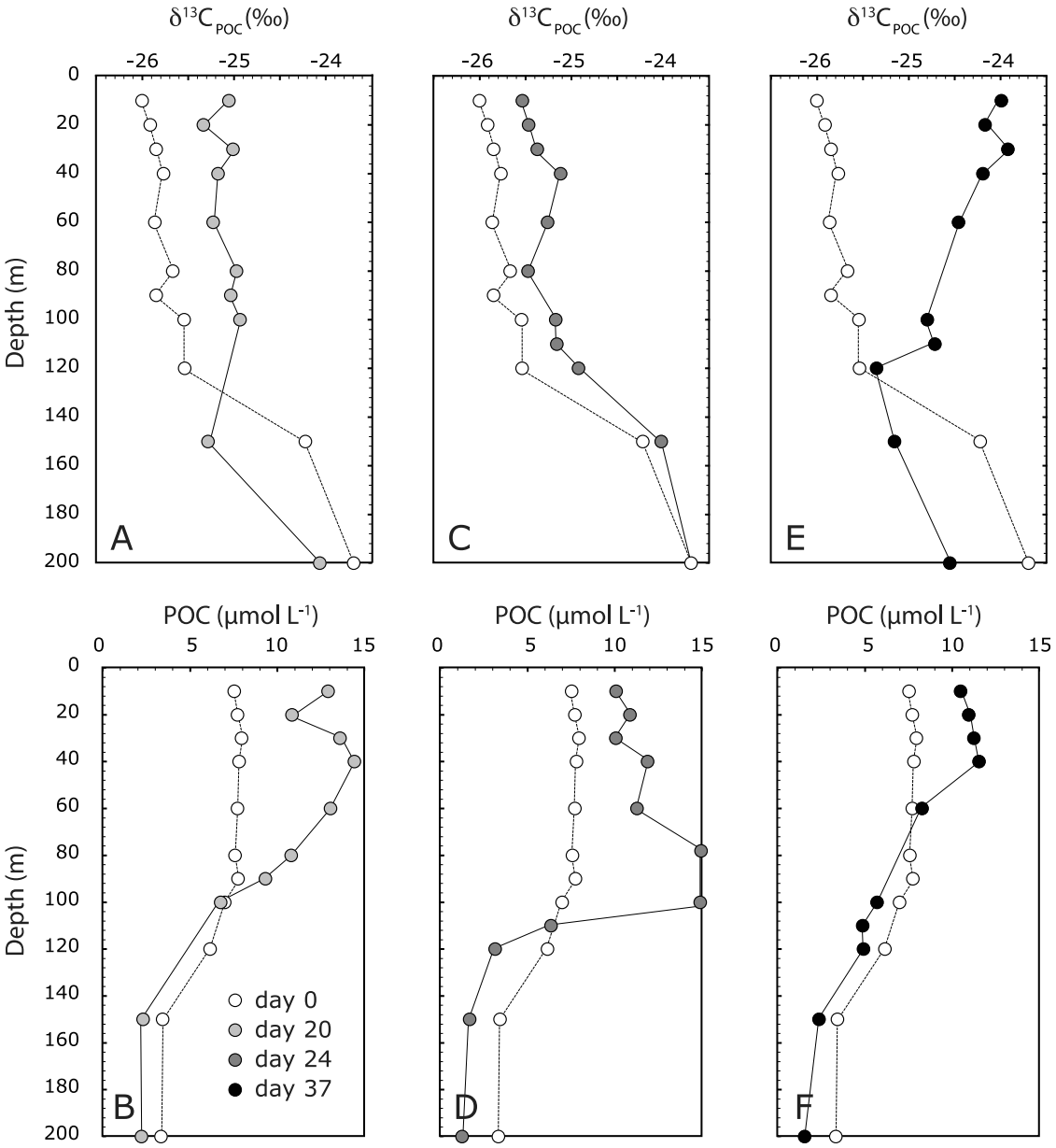

Figure 5. Comparative (a, c, e) $\delta^{13}C_{POC}$ and (b, d, f) POC depth profiles on day 0 (open circles), day 20 (light gray circles; first $\delta^{13}C_{POC}$ peak), day 24 (dark gray circles; $\delta^{13}C_{POC}$ minimum), and day 37 (black circles; second $\delta^{13}C_{POC}$ maximum).

trend line (Figure 6). The first community was dominated by *Chaetoceros* sp. whereas the second community was a mix of cells, including smaller diatoms such as *Pseudo-Nitzchia* sp., *Fragilariopsis cylindrus*, the haptophyte *Phaeocystis antarctica* and several species of picoplankton [*Hoffmann et al.*, 2006; *Croot et al.*, 2007]. Not all the samples fell along these two trend lines. Two of the stations, sampled on days 2 and 11, fell between the main isotope trend lines, suggesting that the phytoplankton were evenly composed of the *Chaetoceros* sp. that would eventually dominate the community and the phytoplankton community that was dominant pre-Fe addition. Similarly, the communities sampled during the period of time following the decline of the *Chaetoceros* assemblage, on days 24 and 26, also fell between the main isotope trend lines, suggesting that these communities were composed of a mixture of phytoplankton from the declining *Chaetoceros* assemblage and the exponentially growing mixed diatom/haptophyte assemblage (Figure 6). A surprising aspect of the grouping of the stations along these two main trend lines was that the pre-Fe addition, or t_0 station, and a low biomass station sampled on day 6, grouped together with the mixed diatom/haptophyte phytoplankton community (Figure 6).

[23] Examining Figure 6, there appeared to be two separate C isotope effects governing the grouping of the data; one effect controlling the 1.56‰ offset in $\delta^{13}C_{POC}$ between the two trend lines ($p < 0.0002$) and a second effect controlling the gradual increase in $\delta^{13}C_{POC}$ along each line. This increase was 1.46‰ along the lighter trend line, 1.18 ± 0.31‰ of it occurring between days 5 and 20, and 1.81‰

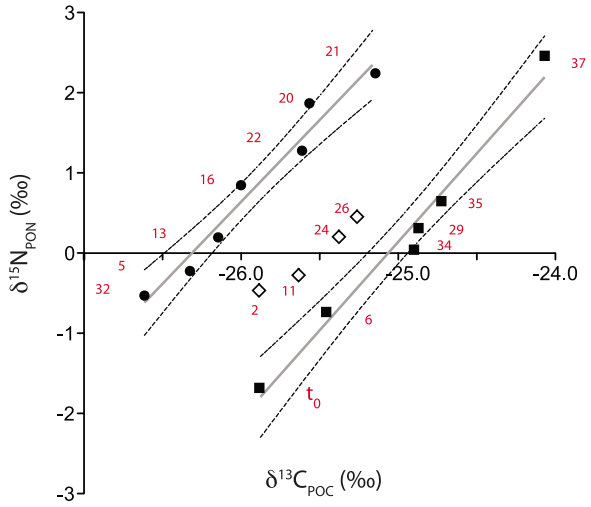

Figure 6. Comparison of $\delta^{15}N_{PON}$ versus $\delta^{13}C_{POC}$ for AML samples. Solid black circles represent stations with assemblages dominated by *Chaetoeros* sp. The slope of the least squares regression line is 2.04 ($r^2 = 0.96$, $p < 0.0002$). Solid black squares represent non-*Chaetoceros*-influenced assemblages. The slope of the least squares regression line is 2.2 ($r^2 = 0.98$, $p < 0.0002$). Dashed lines represent the 95% confidence interval. The difference in C isotope composition between the two regression lines is 1.56 ‰ ($intercept_b$-$intercept_a$) and the difference in N isotope composition is 3.3 ‰ (mean slope*1.56 ‰). Open diamonds represent mixed communities. Numbers in red indicate sampling days.

along the heavier trend line, 0.81 ± 0.13‰ of it occurring between days 29 and 37. The 1.56‰ offset appeared related to a switch between two different states, perhaps controlled by a change in the dominant source of inorganic carbon or in the enzymatic pathway of carbon fixation, whereas the gradual increase in $\delta^{13}C_{POC}$ could be related to source pool dynamics.

[24] It is unlikely the 1.56‰ offset in $\delta^{13}C_{POC}$ between the two communities was mediated by a switch in carbon substrate from CO_2 to HCO_3^-. As mentioned previously, the inorganic C source does not affect particulate ^{13}C enrichment as long as carboxylation by Rubisco is the dominant pathway of carbon fixation in the cell. In this C_3 pathway, HCO_3^- is enzymatically dehydrated to CO_2 via CA, producing light CO_2 (−8.5‰ [*Francois et al.*, 1993]), the substrate for Rubisco. Because of the large isotope discrimination against ^{13}C during carboxylation by Rubisco, this pathway tends toward the lowest $\delta^{13}C_{POC}$ values (−20 to −32‰) regardless of whether CO_2 or HCO_3^- is the original substrate [*Wada and Hattori*, 1991]. In contrast, direct fixation of HCO_3^- into oxaloacetate (OAA) via the action of phosphoenolpyruvate carboxylase (PEPC) and pyruvate carboxylase (PYC) to produce C_4 skeletons for NH_4^+ assimilation is associated with ^{13}C-enriched phytoplankton (−16 to −7‰). This is because the HCO_3^- ion is heavy (1.5‰) and there is very little discrimination against ^{13}C by PEPC [*Guy et al.*, 1989; *Descolas-Gros and Fontugne*, 1990; *Wada and Hattori*, 1991]. The latter pathway, termed hybrid C_3-C_4 metabolism, operates in concert with carboxylation by Rubisco, but varies in importance based on the nitrogen metabolism of the cell [*Turpin and Bruce*, 1990; *Vanlerberghe et al.*, 1990; *Kroth et al.*, 2008]. Based on the difference in C fractionation between Rubisco and PEPC and in the enrichment of their respective substrates (CO_2 and HCO_3^-), the relative activity of these two enzymes should be evident in the ^{13}C enrichment of phytoplankton [*Descolas-Gros and Fontugne*, 1990; *Wada and Hattori*, 1991; *Bentaleb et al.*, 1998]. Here, greater PEPC: Rubisco activity in the second community compared with the first may explain the 1.56‰ difference in $\delta^{13}C_{POC}$ in Figure 6.

[25] The gradual increase in $\delta^{13}C_{POC}$ over time could have resulted from a number of factors affecting the enrichment of CO_2(aq), including air-sea gas exchange, calcification, and depletion of CO_2(aq) by phytoplankton. The air-sea exchange of CO_2 depends on temperature, wind speed, and the pCO_2 gradient between the atmosphere and ocean [*Wanninkhof*, 1992; *Nightingale et al.*, 2000; *Sweeney et al.*, 2007]. As discussed by *Trull and Armand* [2001], the pCO_2 gradient can impact whether air-sea exchange supplies CO_2 that is depleted or enriched in ^{13}C relative to ambient DIC. We used a simple box model [*Long*, 2010] with piston velocities of *Wanninkhof* [1992] to estimate the degree of enrichment of the DIC pool due to primary production and air-sea gas exchange over the course of our experiment. The model was run for 30 days in a 40 m mixed layer with mean net primary production of 20 mmol m^{-2} d^{-1}, initial $\delta^{13}C_{DIC}$ of 1‰, fractionation factor of 18‰, initial DIC of 2135 μmol kg^{-1}, and total alkalinity of 2288 μmol kg^{-1}. The model simulations replicated DIC drawdown over the course of the experiment well (−13.5 μmol kg^{-1} actual and −13 μmol kg^{-1} modeled) at a wind speed of 10 m s^{-1} (EIFEX mean 11 m s^{-1}, high 20 m s^{-1} [*Cisewski et al.*, 2008]). Holding productivity constant, $\delta^{13}C_{DIC}$ increased by 0.015–0.05‰ and $\delta^{13}CO_2$ by 0.13–0.43‰ over a range of wind speeds (0–20 m s^{-1}). Under less extreme forcing, representative of conditions during EIFEX, the simulations show that the effect of gas exchange on the $\delta^{13}C_{POC}$ is negligible.

[26] The change in $\delta^{13}C_{POC}$ due to calcification was probably even smaller than that elicited by air-sea exchange, based on the low initial abundance (6% or less of total community Chl *a* concentration) and fourfold decrease in absolute abundance of the coccolithophore *Emiliania huxleyi* over the course of our experiment [*Hoffmann et al.*, 2006]. Commensurate with the decrease in *E. huxleyi* abundance, total alkalinity increased 4.7 ± 1.5 μmol kg^{-1} and potential alkalinity increased 3.3 ± 1.5 μmol kg^{-1}.

[27] To evaluate possible source pool enrichment due to depletion of CO_2(aq) by phytoplankton, we used a range of published C fractionation factors [e.g., *Francois et al.*, 1993; *Popp et al.*, 1999]. Consistent with closed system dynamics and with the stoichiometry of C:N uptake, the decrease in [CO_2(aq)] was greater than the decrease in [NO_3^-] over the first 29 days of the experiment (Figure 7a). Moreover, the magnitude of change in $\delta^{13}C_{CO2}$ was similar to that of $\delta^{13}C_{POC}$, indicating that enrichment of the source pool could have contributed to the enrichment of the particulate pool prior to day 29 (Figure 7b). Between days 29–37, $\delta^{13}C_{CO2}$ and $\delta^{13}C_{POC}$ became uncoupled due to the large increase in $\delta^{13}C_{POC}$, indicating a shift in the mode of inorganic carbon

acquisition from the preceding period (Figure 7b). During the time of $\delta^{13}C_{POC}$ increase, there was a sharp but transient dip on day 32 (Figure 7b) that coincided with the commencement of the main sedimentation event on days 32–34. During that time, POC export flux at 150 m increased to 130 mmol C $m^{-2}d^{-1}$, up from a background rain rate of 20–30 mmol C $m^{-2}d^{-1}$. After day 34, export fluxes decreased to 10 mmol C $m^{-2}d^{-1}$ for the remainder of the experiment [*Jacquet et al.*, 2008; N. Savoye, unpublished data, 2004]. On day 32, $\delta^{13}C_{POC}$ in the AML decreased by 1.74‰ to the level before iron addition (Figure 7b). Most of the material sinking between days 32–34 originated from a depth of 60–100 m and should not have affected $\delta^{13}C_{POC}$ in the top 40 m. Indeed, the associated decrease in POC in the AML accounted for only 18% of the decrease in $\delta^{13}C_{POC}$ and occurred after day 32. Therefore, the reduction in $\delta^{13}C_{POC}$ on day 32 may have been a continuation of the process of membrane disruption and leakage within the *Chaetoceros* population observed on day 24. This is consistent with observations showing that the *Chaetoceros* cells on day 32 were in a more advanced stage of senescence than on day 24 [*Hoffmann et al.*, 2006; Assmy et al.,

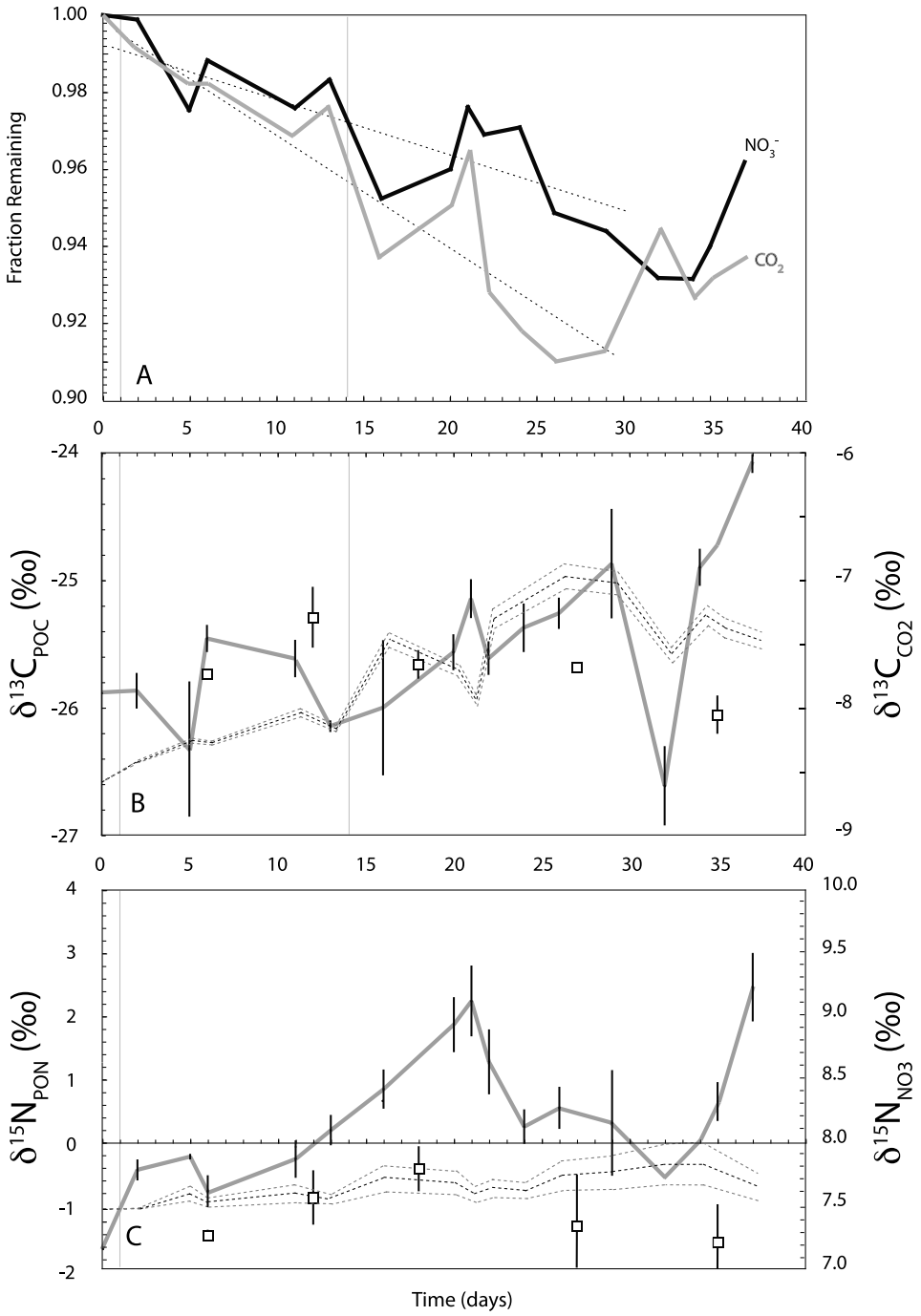

Figure 7

manuscript in preparation, 2011] and may also explain why the $\delta^{13}C/\delta^{15}N$ ratio of this station was similar to that of the first bloom shown in Figure 6.

[28] In contrast to the particulate C signal, the change in $\delta^{15}N_{PON}$ was eight times greater than the change in $\delta^{15}N$ of the NO_3^- pool, excluding enrichment of the substrate pool as the driving force behind the increase in the $\delta^{15}N_{PON}$ for both communities (Figure 7c). A similar eightfold uncoupling between particulate and substrate pool enrichments has been observed in two previous Fe fertilization experiments [*Karsh et al.*, 2003; *Needoba et al.*, 2006]. Although either a change in fractionation associated with NO_3^- assimilation or a switch in N source can produce this result, experimental evidence points to a switch between NH_4^+ as the primary N source before Fe fertilization to NO_3^- as the primary N source following fertilization as the reason for the observed increase in $\delta^{15}N_{PON}$ [*Price et al.*, 1991, 1994; *Needoba et al.*, 2006; *Trull et al.*, 2008]. This is because NH_4^+ has relatively low $\delta^{15}N$ (e.g., −1‰ [*Altabet*, 1988; *Lourey et al.*, 2003]) compared with NO_3^- (e.g., 7.2‰ [*Karsh et al.*, 2003; *DiFiore et al.*, 2006]) in the Southern Ocean.

[29] Given similar increases in $\delta^{15}N_{PON}$ (Figure 6), one might conclude that both communities were dominated by phytoplankton that initially used low-$\delta^{15}N$ NH_4^+ then switched to high-$\delta^{15}N$ NO_3^- as their principal N source. However, there are a number of reasons why the N metabolism of the two different communities was unlikely to be similar. First, we expected NO_3^- uptake rates to decrease toward the latter half of the experiment, commensurate with the decrease in dissolved Fe concentrations [*Maldonado and Price*, 1996, 2000; *Lucas et al.*, 2007]. Dissolved Fe decreased from 2.2 to 0.38 μmol L^{-1} during the *Chaetoceros* bloom and from 0.34 to 0.25 nmol L^{-1} in the last week of the experiment (Schlosser et al., submitted manuscript, 2010). Even in the presence of excess dissolved Fe (dissolved Fe = colloidal + soluble), diatoms will quickly experience Fe limitation during a bloom because organic complexation competes with diatom uptake of soluble Fe [*Wells*, 2003; *Wells et al.*, 2009]. After an initial increase, colloidal ligand concentrations decreased during the latter half of EIFEX, suggesting that the colloids were exported out of the euphotic zone together with particulate material. This implies that iron complexed to the colloids was no longer available at the end of the experiment (Schlosser et al., submitted manuscript, 2010). The $\delta^{15}N_{PON}$ increase in the second community was greatest during the last two stations, at the precise time when dissolved Fe and colloidal ligand concentrations had decreased back to pre-Fe fertilization levels. If this community was able to assimilate the same amount of NO_3^- as the *Chaetoceros*-dominated community, then we see no reason for the high residual NO_3^- concentrations in the Southern Ocean.

[30] Second, larger diatom cells are expected to be the main drivers of NO_3^- uptake based on previous research demonstrating that they out-compete smaller phytoplankton, especially nondiatom phytoplankton, for NO_3^- [*Probyn*, 1985; *Probyn and Painting*, 1985; *Koike et al.*, 1986; *Berg et al.*, 2003; *Lucas et al.*, 2007]. This expectation agrees well with molecular investigations that demonstrate that diatoms have 3–6 copies of NO_3^- transporter genes in their genomes [*Hildebrand and Dahlin*, 2000; *Armbrust et al.*, 2004; *Song and Ward*, 2007] versus 1–2 copies in nondiatom eukaryotic phytoplankton [*Derelle et al.*, 2006; *Song and Ward*, 2007; *Berg et al.*, 2008]. Expression of multiple copies of nearly identical NO_3^- transporter genes may be a means for diatoms to take up NO_3^- at a rate several-fold greater than their competitors [*Hildebrand and Dahlin*, 2000]. Interestingly, in a survey of eukaryotic phytoplankton species, *Song and Ward* [2007] show that expression of NO_3^- transporter genes is greatest in the diatom *Chaetoceros*. This corroborates data from large-scale Fe fertilization experiments where *Chaetoceros* sp. is shown to be the taxa increasing most in abundance following Fe enrichment in 5 out of 9 experiments [*Moore et al.*, 2008]. As such, molecular investigations underscore that Fe promotes the growth of more efficient NO_3^- utilizers, as opposed to promoting NO_3^- utilization in all phytoplankton.

[31] Inconsistent with our expectation that larger diatom cells were the main drivers of NO_3^- uptake, the smallest size fraction in the second community was more enriched in $\delta^{15}N$ than the largest size fraction (Figure 8a). On day 21, the peak of the first bloom, the >20 μm size fraction was close to 6‰ more enriched than the <20 μm size fraction. On day 29, both size fractions were equally enriched, and on the last day of the experiment the <20 μm size fraction was approximately 1.5‰ more enriched than the >20 μm size fraction (Figure 8a). Whereas the discrepancy between the >20 μm and <20 μm size fractions was driven solely by the increase in enrichment of the >20 μm size fraction during the first bloom, the second increase in $\delta^{15}N$ was driven by

Figure 7. (a) Fraction of NO_3^- (black line) or CO_2 (gray line) remaining based on initial concentrations of 24.9 and 19.5 μmol L^{-1}, respectively. Dashed lines represent least squares regression lines through data from day 0 through day 29. After day 29, concentrations of both NO_3^- and CO_2 started to increase. CO_2 was drawn down 1.9 times faster than NO_3^- (CO_2 = −0.003(day) + 1.0, r^2 = 0.86 and NO_3^- = −0.0016(day) + 0.996, r^2 = 0.71). (b) In-patch depth-averaged $\delta^{13}C_{POC}$ (gray line) and change in $\delta^{13}C_{CO2}$ (dashed lines) over the time course. Open squares represent $\delta^{13}C_{POC}$ of out-patch stations. Means and standard deviations of four depths (10–40 m) are shown. The change in $\delta^{13}C_{CO2}$ was calculated as a function of *f*, the fraction of CO_2(aq) remaining, using the equation $\delta^{13}C_{CO2} = \delta^{13}C_{CO2\text{-initial}} - \varepsilon \times \ln(f)$ based on an initial $\delta^{13}C_{CO2}$ of −8.56‰ [*Francois et al.*, 1993] and by varying the isotope fractionation factor ε from 16 to 18‰, spanning a range of ε reported by *Francois et al.* [1993] and *Popp et al.* [1999] for the Southern Ocean. (c) In-patch depth-averaged $\delta^{15}N_{PON}$ (gray line) and change in $\delta^{15}N_{NO3}$ (dashed lines) over the time course. Open squares represent $\delta^{15}N_{PON}$ of out-patch stations. Means and standard deviations of four depths (10–40 m) are shown. The change in $\delta^{15}N_{NO3}$ as a function of *f*, the fraction of NO_3^- remaining, was calculated using the equation $\delta^{15}N_{NO3} = \delta^{15}N_{NO3\text{-initial}} - \varepsilon \times \ln(f)$ based on an initial NO_3^- enrichment of 7.2‰ [*Karsh et al.*, 2003] and by varying the isotope fractionation factor ε from 2.75 to 7.25‰, spanning a range of ε reported in the literature [*Wada and Hattori*, 1978; *Montoya and McCarthy*, 1995; *Altabet and Francois*, 2001; *Karsh et al.*, 2003]. Vertical gray lines in Figures 7a–7c indicate days of iron fertilization.

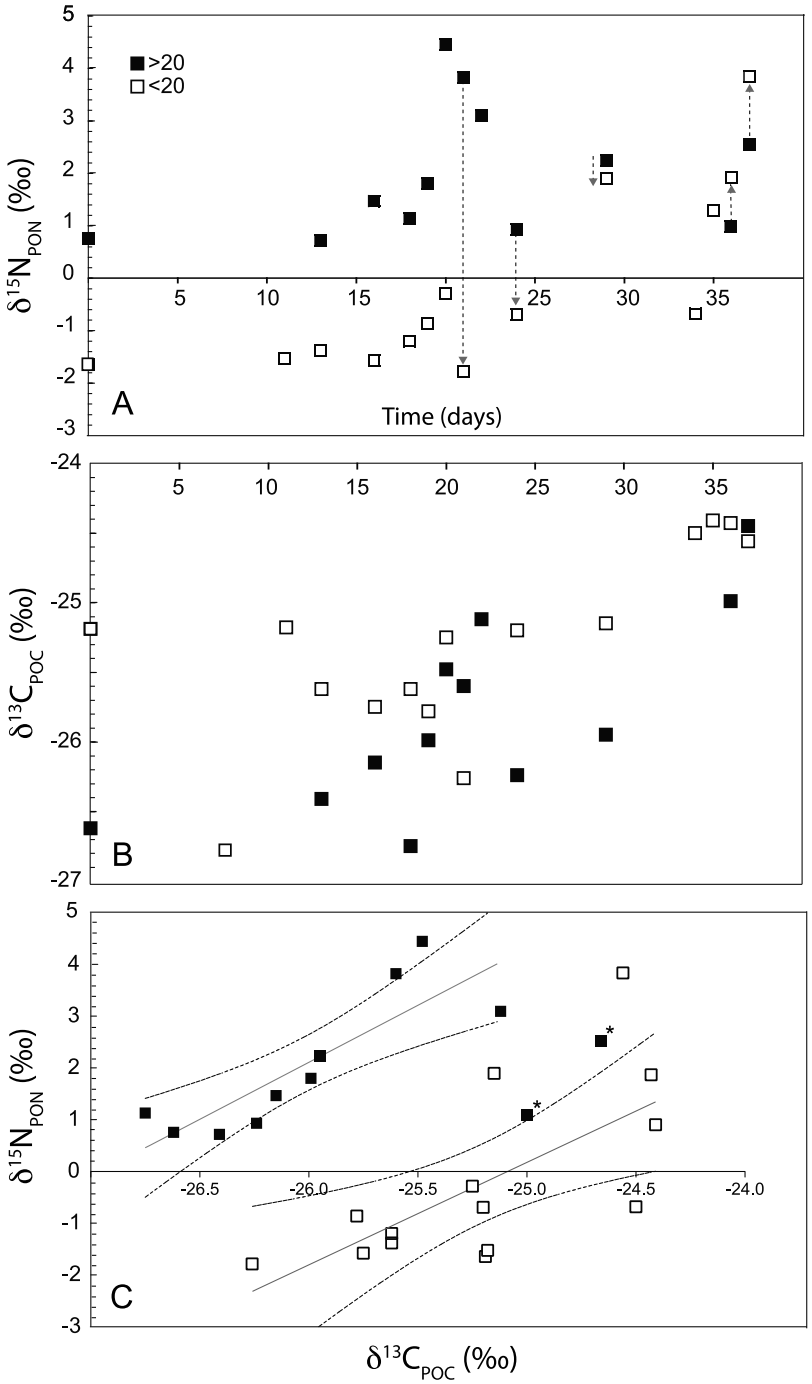

Figure 8. (a) Plot of $\delta^{15}N_{PON}$ for >20 μm (solid black square) and <20 μm (open square) size fractions at 20 m depth. Gray lines emphasize magnitude of difference in $\delta^{15}N$ between the size fractions, and arrowhead indicates the direction from large to small size fraction. (b) Plot of $\delta^{13}C_{POC}$ for >20 μm (solid black square) and <20 μm (open square) size fractions at 20 m depth. (c) Comparison of $\delta^{15}N_{PON}$ versus $\delta^{13}C_{POC}$ for >20 μm and <20 μm size fractions at 20 m depth. The slope of the least squares regression line for the solid black squares representing samples >20 μm is 2.2 ($r^2 = 0.73$, $p < 0.002$). Stars indicate sampling points that were omitted from the linear regression. The slope of the least squares regression line for the open squares representing samples <20 μm is 1.98 ($r^2 = 0.45$, $p < 0.009$). The difference in C isotope composition between the two regression lines is 1.85 ‰.

an increase in both size fractions, albeit the smaller size fraction being more ^{15}N enriched (Figure 8a). In contrast with $\delta^{15}N$, there was no discernible difference among the size fractions with respect to $\delta^{13}C$ (Figure 8b).

[32] The apparent paradox between a decrease in dissolved Fe and an increase in the $\delta^{15}N_{PON}$ of the phytoplankton toward the end of the experiment can potentially be explained by a lower Fe quota for NO_3^- uptake of the second

community [e.g., *Timmermans et al.*, 2004]. This would allow the phytoplankton of the second community to assimilate NO_3^- with less dissolved Fe available in the water column. In addition, the $\delta^{15}N$ of the NO_3^- pool had increased 0.3–0.5‰ by day 29, possibly requiring slightly less uptake of NO_3^- to produce the same level of enrichment compared with the first community. Alternatively, the massive sedimentation event on day 32, preceded by loss of ^{15}N and ^{13}C from the cells (Figures 7b and 7c), could have released ^{15}N-enriched NH_4^+ to the water column that was rapidly taken up by the smaller cells of the community, giving rise to the same level of $\delta^{15}N_{PON}$ enrichment that was attained in the first community. This explanation reconciles the increase in $\delta^{15}N_{PON}$ with a decrease in dissolved Fe concentration and a decrease in NO_3^- drawdown toward the end of the experiment (Figure 7a). However, for this scenario to hold, there must be a minimal difference in the slopes of the $\delta^{15}N/\delta^{13}C$ relationship shown in Figure 6 regardless of whether the cells are assimilating NH_4^+ or NO_3^-. If we assume that NH_4^+-assimilating phytoplankton typically are smaller in size, then we can conclude that the <20 μm size fraction in Figure 8c is dominated by NH_4^+-assimilating phytoplankton and that >20 μm fraction is dominated by NO_3^--assimilating phytoplankton. Because the <20 μm and >20 μm size fractions have the same slope and because we would take the overall slope of all the data in Figure 8c to produce the slopes in Figure 6, one possible interpretation is that assimilation of different N substrates does not affect the slope of the $\delta^{15}N/\delta^{13}C$ relationship of particulate matter to a great extent.

[33] Regardless of the nitrogen source assimilated by the two communities in this experiment, it appears they were separated mainly by the offset in $\delta^{13}C_{POC}$ (Figure 6). The most striking feature of these data is the high $\delta^{15}N_{PON}$ coupled with low $\delta^{13}C_{POC}$ that we observed in the *Chaetoceros*-dominated community. This enrichment pattern appears at first to contradict previous investigations demonstrating enrichment in both $\delta^{13}C_{POC}$ and $\delta^{15}N_{PON}$ with increased NO_3^- utilization in Fe-fertilized water [cf. *Trull et al.*, 2008]. However, by comparing an Fe-depleted station with an Fe-fertilized station from the present investigation, i.e., the t_0 station with day 21, we see that the *Chaetoceros* station is more enriched in both $\delta^{13}C_{POC}$ and $\delta^{15}N_{PON}$ than the t_0 station (−25.1‰ $\delta^{13}C_{POC}$ and 2.2‰ $\delta^{15}N_{PON}$ versus −25.9‰ $\delta^{13}C_{POC}$ and −1.7‰ $\delta^{15}N_{PON}$, respectively) due to the progressive enrichment $\delta^{13}C_{CO2}$ over the course of the bloom. If there was no progressive enrichment in $\delta^{13}C_{CO2}$, then the $\delta^{13}C_{POC}$ of the Fe-depleted water would be greater than the $\delta^{13}C_{POC}$ of the Fe-fertilized water, similar to comparing station t_0 with day 5 (−25.9‰ $\delta^{13}C_{POC}$ and −1.7‰ $\delta^{15}N_{PON}$ versus −26.3‰ $\delta^{13}C_{POC}$ and −0.22‰ $\delta^{15}N_{PON}$). That the rapidly growing *Chaetoceros*-dominated community yielded lower $\delta^{13}C_{POC}$ is of interest from a paleoceanographic perspective because $\delta^{13}C$ tends to be lower in Antarctic sediments during the last glacial maximum where remnants of *Chaetoceros* species and their spores are more abundant [*Crosta and Shemesh*, 2002; *Jacot Des Combes et al.*, 2008].

4. Conclusion

[34] The progressive enrichment in particulate $\delta^{15}N$ in the *Chaetoceros*-dominated assemblage is attributed to a switch in assimilation from NH_4^+ with relatively low isotopic enrichment (−1‰) to NO_3^- with relatively high isotopic enrichment (7.2‰). NH_4^+ assimilation potentially played a greater role in the mixed phytoplankton assemblage succeeding the *Chaetoceros* assemblage, based on decreasing dissolved Fe concentrations and on the decreased disappearance of NO_3^-. The *Chaetoceros*-dominated assemblage was characterized by a rapid net community growth rate, rapid biomass accumulation, and a DIC:NO_3^- disappearance ratio close to Redfield. The second assemblage was characterized by 40% lower net community growth rate, lower biomass accumulation, and a DIC:NO_3^- disappearance ratio that was nearly double that of Redfield. While these successive communities could be differentiated based on the aforementioned parameters, they had identical F_v/F_m signatures. This suggests that relief from Fe limitation raises the quantum yield of PSII of all phytoplankton, but that biomass increases are driven primarily by the ability to induce and up-regulate NO_3^- uptake. Despite the many distinguishing biogeochemical features of these two communities, the most striking was the clear difference in particulate $\delta^{13}C$, beyond the effect of the $\delta^{13}C$ of dissolved CO_2. It was manifested in a lighter C isotopic composition of the rapidly growing *Chaetoceros* assemblage than the following community. Although the physiological explanation for this difference is not immediately clear, it offers up tantalizing insight into the coupling of low $\delta^{13}C$ and high $\delta^{15}N$ observed in ice age Antarctic sediments where *Chaetoceros* remnants, including spores, are abundant.

[35] **Acknowledgments.** We thank Captain U. Pahl and the crew of R/V *Polarstern* and the other cruise participants for their support during the cruise. Special thanks to chief scientist V. Smetacek and to Scott Wankel, C. Neill, P. Assmy, B. Cisewski, I. Benner and I Vöge for help with sampling and analyses. We thank two anonymous reviewers for their helpful comments on the manuscript. This research was funded by the German Research Foundation (DFG) grant BE2634/1 to G.M.B.; by a Bjerknes Centre of Climate Research Centre of Excellence Grant and the Norwegian Research Council "Southern Ocean Biogeochemistry: Education and Research" grant 180328 to R.B.; by Belgian Science Policy Office BELCANTO network contracts EV/37/7C, EV/03/7A, SD/CA/03A and the Vrije Universiteit Brussel grant GOA22, and the Research Foundation Flanders contract G.0021.04 to N.S.; by DFG grants CR145/4-1 and CR145/5-1 to P.L.C.; and by NSF grant ANT0732535 to K.R.A.

References

Altabet, M. A. (1988), Variations in nitrogen isotopic composition between sinking and suspended particles: Implications for nitrogen cycling and particle transformation in the open ocean, *Deep Sea Res.*, *35*, 535–554, doi:10.1016/0198-0149(88)90130-6.

Altabet, M. A. (1989), A time-series study of the vertical structure of nitrogen and particle dynamics in the Sargasso Sea, *Limnol. Oceanogr.*, *34*, 1185–1201, doi:10.4319/lo.1989.34.7.1185.

Altabet, M. A. (1996), Nitrogen and carbon isotopic tracers of the source and transformation of particles in the deep sea, in *Particle Flux in the Ocean*, edited by V. Ittekkot, P. Schafer, S. Honjo, and P. J. Depetris, 155 pp., John Wiley, New York.

Altabet, M. A., and R. Francois (2001), Nitrogen isotope biogeochemistry of the Antarctic Polar Frontal Zone at 170W, *Deep Sea Res., Part II*, *48*, 4247–4273, doi:10.1016/S0967-0645(01)00088-1.

Altabet, M. A., and L. F. Small (1990), Nitrogen isotopic ratios in fecal pellets produced by marine zooplankton, *Geochim. Cosmochim. Acta*, *54*, 155–163, doi:10.1016/0016-7037(90)90203-W.

Antia, N. J., B. R. Berland, D. J. Bonin, and S. Y. Maestrini (1975), Comparative evaluation of certain organic and inorganic sources of nitrogen for phototrophic growth of marine microalgae, *J. Mar. Biol. Assoc. U. K.*, *55*, 519–539, doi:10.1017/S0025315400017239.

Armbrust, E. V., et al. (2004), The genome of the diatom *Thalassiosira pseudonana*: Ecology, evolution, and metabolism, *Science*, *306*, 79–86, doi:10.1126/science.1101156.

Arrigo, K. R., D. H. Robinson, D. Worthen, R. B. Dunbar, G. R. DiTullio, M. VanWoert, and M. P. Lizotte (1999), Phytoplankton community structure and the drawdown of nutrients and CO_2 in the Southern Ocean, *Science*, *283*, 365–367, doi:10.1126/science.283.5400.365.

Assmy, P., J. Henjes, C. Klaas, and V. Smetacek (2007), Mechanisms determining species dominance in a phytoplankton bloom induced by the iron fertilization experiment EisenEx in the Southern Ocean, *Deep Sea Res., Part I*, *54*(3), 340–362, doi:10.1016/j.dsr.2006.12.005.

Agustï, S., and M. C. Sanchez (2002), Cell viability in natural phytoplankton communities quantified by a membrane permeability probe, *Limnol. Oceanogr.*, *47*, 818–828, doi:10.4319/lo.2002.47.3.0818.

Avak, H. and B. Fry (1999), EA-IRMS: Precise and accurate measurement of δ^{15}N on <10 μg N, *Finnigan MAT Appl. Flash Rep. G29*, Thermoquest, Egelsbach, Germany.

Behrenfeld, M. J., A. J. Bale, Z. S. Kolber, J. Aiken, and P. G. Falkowski (1996), Confirmation of iron limitation of phytoplankton photosynthesis in the equatorial Pacific Ocean, *Nature*, *383*(6600), 508–511, doi:10.1038/383508a0.

Bentaleb, I., M. Fontugne, C. Descolas-Gros, C. Girardin, A. Mariotti, C. Pierre, C. Brunet, and A. Poisson (1998), Carbon isotopic fractionation by plankton in the southern Indian Ocean: Relationship between δ^{13}C of particulate organic carbon and dissolved carbon dioxide, *J. Mar. Syst.*, *17*(1–4), 39–58, doi:10.1016/S0924-7963(98)00028-1.

Berg, G. M., M. Balode, I. Purina, S. Bekere, C. Bechemin, and S. Y. Maestrini (2003), Plankton community composition in relation to availability and uptake of oxidized and reduced nitrogen, *Aquat. Microb. Ecol.*, *30*(3), 263–274, doi:10.3354/ame030263.

Berg, G. M., J. Shrager, G. Glockner, K. R. Arrigo, and A. R. Grossman (2008), Understanding nitrogen limitation in *Aureococcus anophagefferens* (Pelagophyceae) through cDNA and qRT-PCR analysis, *J. Phycol.*, *44*(5), 1235–1249, doi:10.1111/j.1529-8817.2008.00571.x.

Blain, S., et al. (2007), Effect of natural iron fertilization on carbon sequestration in the Southern Ocean, *Nature*, *446*(7139), 1070–1074, doi:10.1038/nature05700.

Boyd, P., J. A. Berges, and P. J. Harrison (1998), In vitro iron enrichment experiments at iron-rich and -poor sites in the NE subarctic Pacific, *J. Exp. Mar. Biol. Ecol.*, *227*(1), 133–151, doi:10.1016/S0022-0981(97)00264-5.

Boyd, P. W. (2002), The role of iron in the biogeochemistry of the Southern Ocean and equatorial Pacific: A comparison of in situ iron enrichments, *Deep Sea Res., Part II*, *49*(9–10), 1803–1821, doi:10.1016/S0967-0645(02)00013-9.

Boyd, P. W., and E. R. Abraham (2001), Iron-mediated changes in phytoplankton photosynthetic competence during SOIREE, *Deep Sea Res., Part II*, *48*(11–12), 2529–2550, doi:10.1016/S0967-0645(01)00007-8.

Boyd, P. W., et al. (2000), A mesoscale phytoplankton bloom in the polar Southern Ocean stimulated by iron fertilization, *Nature*, *407*(6805), 695–702, doi:10.1038/35037500.

Caldeira, K., and P. B. Duffy (2000), The role of the Southern Ocean in uptake and storage of anthropogenic carbon dioxide, *Science*, *287*(5453), 620–622, doi:10.1126/science.287.5453.620.

Cisewski, B., V. H. Strass, M. Losch, and H. Prandke (2008), Mixed layer analysis of a mesoscale eddy in the Antarctic Polar Front Zone, *J. Geophys. Res.*, *113*, C05017, doi:10.1029/2007JC004372.

Coale, K. H., et al. (1996), A massive phytoplankton bloom induced by an ecosystem-scale iron fertilization experiment in the equatorial Pacific Ocean, *Nature*, *383*, 495–501, doi:10.1038/383495a0.

Coale, K. H., et al. (2004), Southern ocean iron enrichment experiment: Carbon cycling in high- and low-Si waters, *Science*, *304*(5669), 408–414, doi:10.1126/science.1089778.

Croot, P. L., U. Passow, P. Assmy, S. Jansen, and V. H. Strass (2007), Surface active substances in the upper water column during a Southern Ocean Iron Fertilization Experiment (EIFEX), *Geophys. Res. Lett.*, *34*, L03612, doi:10.1029/2006GL028080.

Crosta, X., and A. Shemesh (2002), Reconciling down core anticorrelation of diatom carbon and nitrogen isotopic ratios from the Southern Ocean, *Paleoceanography*, *17*(1), 1010, doi:10.1029/2000PA000565.

Derelle, E., et al. (2006), Genome analysis of the smallest free-living eukaryote *Ostreococcus tauri* unveils many unique features, *Proc. Natl. Acad. Sci. U. S. A.*, *103*(31), 11,647–11,652, doi:10.1073/pnas.0604795103.

Descolas-Gros, C., and M. Fontugne (1990), Stable carbon isotope fractionation by marine phytoplankton during photosynthesis, *Plant Cell Environ.*, *13*(3), 207–218, doi:10.1111/j.1365-3040.1990.tb01305.x.

Deuser, W. G. (1970), Isotopic evidence for diminishing supply of available carbon during diatom bloom in the Black Sea, *Nature*, *225*, 1069–1071, doi:10.1038/2251069a0.

DeYoe, H. R., and C. A. Suttle (1994), The inability of the Texas brown tide alga to use nitrate and the role of nitrogen in the initiation of a persistent bloom of this organism, *J. Phycol.*, *30*(5), 800–806, doi:10.1111/j.0022-3646.1994.00800.x.

Dickson, A. G., and C. Goyet (1994), Handbook of methods for the analysis of the various parameters of the carbon dioxide system in sea water, Version 2, *Tech. Rep. ORNL/CDIAC-74*, Oak Ridge Natl. Lab, Oak Ridge, Tenn.

DiFiore, P. J., D. M. Sigman, T. W. Trull, M. J. Lourey, K. Karsh, G. Cane, and R. Ho (2006), Nitrogen isotope constraints on subantarctic biogeochemistry, *J. Geophys. Res.*, *111*, C08016, doi:10.1029/2005JC003216.

Franck, V. M., K. W. Bruland, D. A. Hutchins, and M. A. Brezezinski (2003), Iron and zinc effects on silicic acid and nitrate uptake kinetics in three high-nutrient, low-chlorophyll (HNLC) regions, *Mar. Ecol. Prog. Ser.*, *252*, 15–33, doi:10.3354/meps252015.

Francois, R., M. A. Altabet, and R. Goericke (1993), Changes in the δ^{13}C of surface water particulate organic matter across the subtropical convergence in the SW Indian Ocean, *Global Biogeochem. Cycles*, *7*(3), 627–644, doi:10.1029/93GB01277.

Francois, R., M. A. Altabet, E. F. Yu, D. M. Sigman, M. P. Bacon, M. Frank, G. Bohrmann, G. Bareille, and L. D. Labeyrie (1997), Contribution of Southern Ocean surface-water stratification to low atmospheric CO_2 concentrations during the last glacial period, *Nature*, *389*(6654), 929–935, doi:10.1038/40073.

Freeman, K. H., and J. M. Hayes (1992), Fractionation of carbon isotopes by phytoplankton and estimates of ancient CO_2 levels, *Global Biogeochem. Cycles*, *6*, 185–198, doi:10.1029/92GB00190.

Geider, R. J., J. La Roche, R. M. Greene, and M. Olaizola (1993), Response of the photosynthetic apparatus of *Phaeodactylum tricornutum* (Bacillariophyceae) to nitrate, phosphate, or iron starvation, *J. Phycol.*, *29*(6), 755–766, doi:10.1111/j.0022-3646.1993.00755.x.

Gervais, F., U. Riebesell, and M. Y. Gorbunov (2002), Changes in primary productivity and chlorophyll a in response to iron fertilization in the Southern Polar Frontal Zone, *Limnol. Oceanogr.*, *47*(5), 1324–1335, doi:10.4319/lo.2002.47.5.1324.

Gille, S. T. (2002), Warming of the Southern Ocean since the 1950s, *Science*, *295*(5558), 1275–1277, doi:10.1126/science.1065863.

Graziano, L. M., J. La Roche, and R. J. Geider (1996), Physiological responses to phosphorus limitation in batch and steady-state cultures of *Dunaliella tertiolecta* (Chlorophyta): A unique stress protein as an indicator of phosphate deficiency, *J. Phycol.*, *32*, 825–838, doi:10.1111/j.0022-3646.1996.00825.x.

Greene, R. M., R. J. Geider, and P. G. Falkowski (1991), Effect of iron limitation on photosynthesis in a marine diatom, *Limnol. Oceanogr.*, *36*(8), 1772–1782, doi:10.4319/lo.1991.36.8.1772.

Guy, R. D., G. C. Vanlerberghe, and D. H. Turpin (1989), Significance of phosphoenolpyruvate carboxylase during ammonium assimilation-carbon isotope discrimination in photosynthesis and respiration by the N-limited green-alga *Selenastrum minutum*, *Plant Physiol.*, *89*(4), 1150–1157, doi:10.1104/pp.89.4.1150.

Hansen, J., et al. (2005), Earth's energy imbalance: Confirmation and implications, *Science*, *308*(5727), 1431–1435, doi:10.1126/science.1110252.

Hildebrand, M., and K. Dahlin (2000), Nitrate transporter genes from the diatom *Cylindrotheca fusiformis* (Bacillariophyceae): mRNA levels controlled by nitrogen source and by the cell cycle, *J. Phycol.*, *36*(4), 702–713, doi:10.1046/j.1529-8817.2000.99153.x.

Hiscock, M. R., V. P. Lance, A. M. Apprill, R. R. Bidigare, Z. I. Johnson, B. G. Mitchell, W. O. Smith, and R. T. Barber (2008), Photosynthetic maximum quantum yield increases are an essential component of the Southern Ocean phytoplankton response to iron, *Proc. Natl. Acad. Sci. U. S. A.*, *105*(12), 4775–4780, doi:10.1073/pnas.0705006105.

Hoffmann, L. J., I. Peeken, K. Lochte, P. Assmy, and M. Veldhuis (2006), Different reactions of Southern Ocean phytoplankton size classes to iron fertilization, *Limnol. Oceanogr.*, *51*(3), 1217–1229, doi:10.4319/lo.2006.51.3.1217.

Jacot Des Combes, H., O. Esper, C. L. De La Rocha, A. Abelmann, R. Gersonde, R. Yam, and A. Shemesh (2008), Diatom δ^{13}C, δ^{15}N, and C/N since the last glacial maximum in the Southern Ocean: Potential impacts of species composition, *Paleoceanography*, *23*, PA4209, doi:10.1029/2008PA001589.

Jacquet, S. H. M., N. Savoye, F. Dehairs, V. H. Strass, and D. Cardinal (2008), Mesopelagic carbon remineralization during the European iron fertilization experiment, *Global Biogeochem. Cycles*, *22*, GB1023, doi:10.1029/2006GB002902.

Johnson, K. M., P. J. Williams, L. Brandstrom, and J. MN. Sieburth (1987), Coulometric total carbon analysis for marine studies: Automation and calibration, *Mar. Chem.*, *21*, 117–133, doi:10.1016/0304-4203(87)90033-8.

Karsh, K. L., T. W. Trull, A. J. Lourey, and D. M. Sigman (2003), Relationship of nitrogen isotope fractionation to phytoplankton size and iron availability during the Southern Ocean Iron RElease Experiment (SOIREE), *Limnol. Oceanogr.*, *48*(3), 1058–1068, doi:10.4319/lo.2003.48.3.1058.

Khatiwala, S., F. Primeau, and T. Hall (2009), Reconstruction of the history of anthropogenic CO_2 concentrations in the ocean, *Nature*, *462*(7271), 346–349, doi:10.1038/nature08526.

Koike, I., O. Holmhansen, and D. C. Biggs (1986), Inorganic nitrogen-metabolism by Antarctic phytoplankton with special reference to ammonium cycling, *Mar. Ecol. Prog. Ser.*, *30*(2–3), 105–116, doi:10.3354/meps030105.

Kolber, Z., J. Zehr, and P. G. Falkowski (1988), Effects of growth irradiance and nitrogen limitation on photosynthetic energy conversion in photosystem II, *Plant Physiol.*, *88*, 923–929, doi:10.1104/pp.88.3.923.

Kolber, Z. S., et al. (1994), Iron limitation of phytoplankton photosynthesis in the equatorial Pacific Ocean, *Nature*, *371*, 145–149, doi:10.1038/371145a0.

Krägefsky, S., U. Bathmann, V. Strass, and D. Wolf-Gladrow (2009), Responses of small copepods to an iron-induced phytoplankton bloom: A model to address the mechanisms of aggregation, *Mar. Ecol. Prog. Ser.*, *374*, 181–198, doi:10.3354/meps07761.

Kroth, P. G., et al. (2008), A model for carbohydrate metabolism in the diatom *Phaeodactylum tricornutum* deduced from comparative whole genome analysis, *PLoS ONE*, *3*, e1426, doi:10.1371/journal.pone.0001426.

La Roche, J., R. J. Geider, L. M. Graziano, H. Murray, and K. Lewis (1993), Induction of specific proteins in eukaryotic algae grown under iron-deficient, phosphorus-deficient, or nitrogen-deficient conditions, *J. Phycol.*, *29*(6), 767–777, doi:10.1111/j.0022-3646.1993.00767.x.

La Roche, J., P. W. Boyd, R. M. L. McKay, and R. J. Geider (1996), Flavodoxin as an in situ marker for iron stress in phytoplankton, *Nature*, *382*(6594), 802–805, doi:10.1038/382802a0.

Long, M. C. (2010), Upper ocean physical and ecological dynamics in the Ross Sea, Antarctica, Ph.D. thesis, Stanford Univ., Stanford, Calif.

Lorrain, A., N. Savoye, L. Chauvaud, Y. M. Paulet, and N. Naulet (2003), Decarbonation and preservation method for the analysis of organic C and N contents and stable isotope ratios of low-carbonated suspended particulate material, *Anal. Chim. Acta*, *491*(2), 125–133, doi:10.1016/S0003-2670(03)00815-8.

Lourey, M. J., T. W. Trull, and D. M. Sigman (2003), Sensitivity of $\delta^{15}N$ of nitrate, surface suspended and deep sinking particulate nitrogen to seasonal nitrate depletion in the Southern Ocean, *Global Biogeochem. Cycles*, *17*(3), 1081, doi:10.1029/2002GB001973.

Lucas, M., S. Seeyave, R. Sanders, C. M. Moore, R. Williamson, and M. Stinchcombe (2007), Nitrogen uptake responses to a naturally Fe-fertilised phytoplankton bloom during the 2004/2005 CROZEX study, *Deep Sea Res., Part II*, *54*(18–20), 2138–2173, doi:10.1016/j.dsr2.2007.06.017.

Maldonado, M. T., and N. M. Price (1996), Influence of N substrate on Fe requirements of marine centric diatoms, *Mar. Ecol. Prog. Ser.*, *141*, 161–172, doi:10.3354/meps141161.

Maldonado, M. T., and N. M. Price (2000), Nitrate regulation of Fe reduction and transport by Fe-limited *Thalassiosira oceanica*, *Limnol. Oceanogr.*, *45*(4), 814–826, doi:10.4319/lo.2000.45.4.0814.

Marinov, I., A. Gnanadesikan, J. R. Toggweiler, and J. L. Sarmiento (2006), The Southern Ocean biogeochemical divide, *Nature*, *441*(7096), 964–967, doi:10.1038/nature04883.

Martin, J. H. (1990), Glacial-interglacial CO_2 change: The iron hypothesis, *Paleoceanography*, *5*, 1–13, doi:10.1029/PA005i001p00001.

Mikaloff Fletcher, S. E. M., et al. (2006), Inverse estimates of anthropogenic CO_2 uptake, transport, and storage by the ocean, *Global Biogeochem. Cycles*, *20*(2), GB2002, doi:10.1029/2005GB002530.

Montoya, J. P., and J. J. McCarthy (1995), Isotopic fractionation during nitrate uptake by phytoplankton grown in continuous culture, *J. Plankton Res.*, *17*(3), 439–464, doi:10.1093/plankt/17.3.439.

Moore, C. M., M. M. Mills, A. Milne, R. Langlois, E. P. Achterberg, K. Lochte, R. J. Geider, and J. La Roche (2006), Iron limits primary productivity during spring bloom development in the central North Atlantic, *Global Change Biol.*, *12*(4), 626–634, doi:10.1111/j.1365-2486.2006.01122.x.

Moore, L. R., A. F. Post, G. Rocap, and S. W. Chisholm (2002), Utilization of different nitrogen sources by the marine cyanobacteria *Prochlorococcus* and *Synechococcus*, *Limnol. Oceanogr.*, *47*(4), 989–996, doi:10.4319/lo.2002.47.4.0989.

Moore, S. K., V. L. Trainer, N. J. Mantua, M. S. Parker, E. A. Laws, L. C. Backer, and L. E. Fleming (2008), Impacts of climate variability and future climate change on harmful algal blooms and human health, *Environ. Health*, *7*, S4, doi:10.1186/1476-069X-7-S2-S4.

Morris, P. J., R. Sanders, R. Turnewitsch, and S. Thomalla (2007), ^{234}Th-derived particulate organic carbon export from an island-induced phytoplankton bloom in the Southern Ocean, *Deep Sea Res., Part II*, *54*(18–20), 2208–2232, doi:10.1016/j.dsr2.2007.06.002.

Needoba, J. A., A. Marchetti, M. F. Henry, P. J. Harrison, C. S. Wong, W. K. Johnson, and T. F. Pedersen (2006), Stable nitrogen isotope dynamics of a mesoscale iron enrichment experiment in the NE Subarctic Pacific, *Deep Sea Res., Part II*, *53*(20–22), 2214–2230, doi:10.1016/j.dsr2.2006.05.021.

Nightingale, P. D., P. S. Liss, and P. Schlosser (2000), Measurements of air-sea gas transfer during an open ocean algal bloom, *Geophys. Res. Lett.*, *27*, 2117–2120, doi:10.1029/2000GL011541.

Pollard, R. T., et al. (2009), Southern Ocean deep-water carbon export enhanced by natural iron fertilization, *Nature*, *457*(7229), 577–580, doi:10.1038/nature07716.

Popp, B. N., R. Takigiku, J. M. Hayes, J. W. Louda, and E. W. Baker (1989), The post-Paleozoic chronology and mechanism of ^{13}C depletion in primary marine organic matter, *Am. J. Sci.*, *289*(4), 436–454, doi:10.2475/ajs.289.4.436.

Popp, B. N., et al. (1999), Controls on the carbon isotopic composition of Southern Ocean phytoplankton, *Global Biogeochem. Cycles*, *13*(4), 827–844, doi:10.1029/1999GB900041.

Price, N. M., L. F. Andersen, and F. M. M. Morel (1991), Iron and nitrogen nutrition of equatorial Pacific plankton, *Deep-Sea Res.*, *38*(11), 1361–1378, doi:10.1016/0198-0149(91)90011-4.

Price, N. M., B. A. Ahner, and F. M. M. Morel (1994), The equatorial Pacific-Ocean: Grazer-controlled phytoplankton populations in an iron-limited ecosystem, *Limnol. Oceanogr.*, *39*(3), 520–534, doi:10.4319/lo.1994.39.3.0520.

Probyn, T. A. (1985), Nitrogen uptake by size-fractionated phytoplankton populations in the southern Benguela upwelling system, *Mar. Ecol. Prog. Ser.*, *22*(3), 249–258, doi:10.3354/meps022249.

Probyn, T. A., and S. J. Painting (1985), Nitrogen uptake by size-fractionated phytoplankton populations in Antarctic surface waters, *Limnol. Oceanogr.*, *30*(6), 1327–1332, doi:10.4319/lo.1985.30.6.1327.

Rau, G. H., T. Takahashi, and D. J. D. Marais (1989), Latitudinal variations in plankton $\delta^{13}C$: Implications for CO_2 and productivity in past oceans, *Nature*, *341*(6242), 516–518, doi:10.1038/341516a0.

Rau, G. H., J. L. Teyssie, F. Rassoulzadegan, and S. W. Fowler (1990), $^{13}C/^{12}C$ and $^{15}N/^{14}N$ variations among size-fractionated marine particles: Implications for their origin and trophic relationships, *Mar. Ecol. Prog. Ser.*, *59*(1–2), 33–38, doi:10.3354/meps059033.

Rau, G. H., T. Takahashi, D. J. Desmarais, D. J. Repeta, and J. H. Martin (1992), The relationship between $\delta^{13}C$ of organic matter and $[CO_2(aq)]$ in ocean surface water: Data from a JGOFS site in the northeast Atlantic Ocean and a model, *Geochim. Cosmochim. Acta*, *56*(3), 1413–1419, doi:10.1016/0016-7037(92)90073-R.

Raven, J. A. (1988), The iron and molybdenum use efficicencies of plant growth with different energy, carbon and nitrogen sources, *New Phytol.*, *109*, 279–287, doi:10.1111/j.1469-8137.1988.tb04196.x.

Riebesell, U., and D. Wolf-Gladrow (1995), Growth limits on phytoplankton, *Nature*, *373*(6509), 28–28, doi:10.1038/373028b0.

Röttgers, R., F. Colijn, and M. Dibbern (2005), Algal physiology and biooptics, *Rep. Polar Mar. Res.*, *500*, 82–88.

Savoye, N., T. W. Trull, S. H. M. Jacquet, J. Navez, and F. Dehairs (2008), ^{234}Th-based export fluxes during a natural iron fertilization experiment in the Southern Ocean (KEOPS), *Deep Sea Res., Part II*, *55*(5–7), 841–855, doi:10.1016/j.dsr2.2007.12.036.

Seeyave, S., M. I. Lucas, C. M. Moore, and A. J. Poulton (2007), Phytoplankton productivity and community structure in the vicinity of the Crozet Plateau during austral summer 2004/2005, *Deep Sea Res., Part II*, *54*(18–20), 2020–2044, doi:10.1016/j.dsr2.2007.06.010.

Sigman, D. M., and E. A. Boyle (2000), Glacial/interglacial variations in atmospheric carbon dioxide, *Nature*, *407*(6806), 859–869, doi:10.1038/35038000.

Sigman, D. M., and K. L. Casciotti (2001), Nitrogen isotopes in the ocean, in *Encyclopedia of Ocean Sciences*, edited by J. H. Steele, S. A. Thorpe, and K. K. Turekian, pp. 1884–1894, Academic, San Diego, Calif., doi:10.1006/rwos.2001.0172

Sigman, D. M., M. A. Altabet, R. Francois, D. C. McCorkle, and J. F. Gaillard (1999), The isotopic composition of diatom-bound nitrogen in Southern Ocean sediments, *Paleoceanography*, *14*(2), 118–134, doi:10.1029/1998PA900018.

Song, B., and B. B. Ward (2007), Molecular cloning and characterization of high-affinity nitrate transporters in marine phytoplankton, *J. Phycol.*, *43*(3), 542–552, doi:10.1111/j.1529-8817.2007.00352.x.

Strass, V., B. Cisewski, S. Gonzalez, H. Leach, K.-D. Loquay, H. Prandke, H. Rohr, and M. Thomas (2005), The physical setting of the European

Iron Fertilization Experiment 'EIFEX' in the Southern Ocean, *Rep. Polar Mar. Res.*, *500*, 15–46.

Strzepek, R. F., and P. J. Harrison (2004), Photosynthetic architecture differs in coastal and oceanic diatoms, *Nature*, *431*(7009), 689–692, doi:10.1038/nature02954.

Sweeney, C., E. Gloor, A. R. Jacobson, R. M. Key, G. McKinley, J. L. Sarmiento, and R. Wanninkhof (2007), Constraining global air-sea gas exchange for CO_2 with recent bomb ^{14}C measurements, *Global Biogeochem. Cycles*, *21*, GB2015, doi:10.1029/2006GB002784.

Takahashi, T., et al. (2002), Global sea-air CO_2 flux based on climatological surface ocean pCO_2, and seasonal biological and temperature effects, *Deep Sea Res., Part II*, *49*(9–10), 1601–1622, doi:10.1016/S0967-0645(02)00003-6.

Tamelander, T., C. Kivimae, R. G. J. Bellerby, P. E. Renaud, and S. Kristiansen (2009), Base-line variations in stable isotope values in an Arctic marine ecosystem: Effects of carbon and nitrogen uptake by phytoplankton, *Hydrobiologia*, *630*(1), 63–73, doi:10.1007/s10750-009-9780-2.

Timmermans, K. R., B. van der Wagt, and H. J. W. de Baar (2004), Growth rates, half-saturation constants, and silicate, nitrate, and phosphate depletion in relation to iron availability of four large, open-ocean diatoms from the Southern Ocean, *Limnol. Oceanogr.*, *49*, 2141–2151, doi:10.4319/lo.2004.49.6.2141.

Timmermans, K. R., M. J. W. Veldhuis, and C. P. D. Brussard (2007), Cell death in three marine diatom species in response to different irradiance levels, silicate or iron concentrations, *Aquat. Microb. Ecol.*, *46*, 253–261, doi:10.3354/ame046253.

Tortell, P. D., J. R. Reinfelder, and F. M. M. Morel (1997), Active uptake of bicarbonate by diatoms, *Nature*, *390*, 243–244, doi:10.1038/36765.

Tortell, P. D., C. Payne, C. Gueguen, R. F. Strzepek, P. W. Boyd, and B. Rost (2008), Inorganic carbon uptake by Southern Ocean phytoplankton, *Limnol. Oceanogr.*, *53*(4), 1266–1278, doi:10.4319/lo.2008.53.4.1266.

Trull, T. W., and L. Armand (2001), Insights into Southern Ocean carbon export from the $\delta^{13}C$ of particles and dissolved inorganic carbon during the SOIREE iron release experiment, *Deep Sea Res., Part II*, *48*, 2655–2680, doi:10.1016/S0967-0645(01)00013-3.

Trull, T. W., D. Davies, and K. Casciotti (2008), Insights into nutrient assimilation and export in naturally iron-fertilized waters of the Southern Ocean from nitrogen, carbon and oxygen isotopes, *Deep Sea Res., Part II*, *55*(5–7), 820–840, doi:10.1016/j.dsr2.2007.12.035.

Turpin, D. H., and D. Bruce (1990), Regulation of photosynthetic light harvesting by nitrogen assimilation in the green-alga *Selenastrum minutum*, *FEBS Lett.*, *263*(1), 99–103, doi:10.1016/0014-5793(90)80714-T.

Vanlerberghe, G. C., K. A. Schuller, R. G. Smith, R. Feil, W. C. Plaxton, and D. H. Turpin (1990), Relationship between NH_4^+ assimilation rate and in vivo phosphoenolpyruvate carboxylase activity, *Plant Physiol.*, *94*, 284–290, doi:10.1104/pp.94.1.284.

Villinski, J. C., J. M. Hayes, S. C. Brassell, V. L. Riggert, and R. B. Dunbar (2008), Sedimentary sterols as biogeochemical indicators in the Southern Ocean, *Org. Geochem.*, *39*(5), 567–588, doi:10.1016/j.orggeochem.2008.01.009.

Wada, E., and A. Hattori (1978), Nitrogen isotope effects in the assimilation of inorganic nitrogenous compounds by marine diatoms, *Geomicrobiol. J.*, *1*, 85–101, doi:10.1080/01490457809377725.

Wada, E., and A. Hattori (1991), Variation of $^{15}N/^{14}N$ in nitrogen cycling and its significance in marine environments, in *Nitrogen in the Sea: Forms, Abundances, and Rate Processes*, edited by E. Wada and A. Hattori, pp. 141–176, CRC Press, Boca Raton, Fla.

Wanninkhof, R. (1992), Relationship between wind speed and gas exchange over the ocean, *J. Geophys. Res.*, *97*, 7373–7382, doi:10.1029/92JC00188.

Watson, A., D. Bakker, A. Ridgwell, P. Boyd, and C. Law (2000), Effect of iron supply on Southern Ocean CO_2 uptake and implications for glacial atmospheric CO_2, *Nature*, *407*(6805), 730–733, doi:10.1038/35037561.

Wells, M. L. (2003), The level of iron enrichment required to initiate diatom blooms in HNLC waters, *Mar. Chem.*, *82*(1–2), 101–114, doi:10.1016/S0304-4203(03)00055-0.

Wells, M. L., C. G. Trick, W. P. Cochlan, and B. Beall (2009), Persistence of iron limitation in the western subarctic Pacific SEEDS II mesoscale fertilization experiment, *Deep Sea Res., Part II*, *56*(26), 2810–2821, doi:10.1016/j.dsr2.2009.06.007.

K. R. Arrigo, G. M. Berg, M. C. Long, and M. M. Mills, Environmental Earth System Science, Stanford University, 397 Panama Mall, Stanford, CA 94305, USA. (mine.berg@gmail.com)

R. Bellerby, Bjerknes Center for Climate Research, University of Bergen, Allégaten 55, NL-5007 Bergen, Norway.

P. L. Croot, Plymouth Marine Laboratory, Marine Biogeochemistry, Prospect Place, Plymouth PL1 3DH, UK.

R. Röttgers, Forschungszentrum Geesthacht, Institut für Küstenforschung, Max-Planck-Straße 1, D-21502 Geesthacht, Germany.

N. Savoye, UMR 5805 EPOC, Station Marine d'Arcachon, Université Bordeaux 1/CNRS, 2 Rue du Professeur Jolyet, F-33120 Arcachon CEDEX, France.

V. Strass, Alfred Wegener Institute for Polar and Marine Research, PO Box 120161, D-27515 Bremerhaven, Germany.

A. Webb, Oceanography Department, University of Cape Town, Private Bag X3, Rondebosch, South Africa.